

THE CYCLIC SIEVING PHENOMENON AND FRIEZE PATTERNS

ASHLEIGH ADAMS AND ESTHER BANAIAH

ABSTRACT. We exhibit two instances of the cyclic sieving phenomenon - one on dissections of a polygon of a fixed type and one on triangulations of a once-punctured polygon. We use these results to give refined enumerations of certain families of frieze patterns. We also give an interpretation of finite, positive integral frieze patterns fixed under nontrivial rotations as frieze patterns from a family of orbifolds and show that these are always unitary. Finally, we give a bijection between Holm–Jørgensen frieze patterns and p -Dyck paths, extending a recent construction of Cañadas, Gaviria, Rios, and Espinosa, and discuss an induced rotation map on Dyck paths. Several conjectures and questions for future study are highlighted throughout the article.

1. INTRODUCTION

Sets of noncrossing diagonals on polygons (i.e. *dissections* or partial triangulations) are a fundamental object in many branches of combinatorics. Enumerating such sets with various constraints, such as the number of diagonals used or the types of faces cut out by the diagonals, often proves to be an interesting problem, as was pointed out by Cayley over 100 years ago [Cay90]. For a small sample of the many such enumerative formulas, see [Bec98, Kir57, PS00, Sta96]. Sets with the maximal possible number of noncrossing diagonals, i.e. triangulations, are of particular interest as they are enumerated by the ubiquitous Catalan numbers.

The slogan of combinatorics is often that it is the “study of counting”, but in practice many interesting problems in combinatorics concern the symmetries underlying a set as well. This approach even has interdisciplinary applications, such as in characterizing polymers [DKK11]. In the case of dissections of a polygon, it is natural to group dissections according to their cyclic equivalence classes. The size of the equivalence class tells us about the symmetry present in the original dissection. Reiner, Stanton, and White defined the *cyclic sieving phenomenon* in order to systemize such a problem.

Definition 1 ([RSW04]). *A triple $(X, G_n, X(q))$ consisting of a set X endowed with the action of a cyclic group of order n , $G_n = \langle \sigma \rangle$, and a polynomial $X(q) \in \mathbb{Z}[q]$ is said to exhibit the cyclic sieving phenomenon if $X(\zeta_n^k)$ is equal to the number of fixed points of σ^k where ζ_n is a primitive n -th root of unity.*

In particular, in order for $(X, G_n, X(q))$ to exhibit CSP, the polynomial $X(q)$ must satisfy $X(\zeta_n^n) = X(1) = |X|$. One striking beauty of the CSP is that often $X(q)$ is a natural q -analogue of an enumeration formula for X . For an excellent survey on the topic, see [Sag11].

In their seminal paper, Reiner, Stanton, and White show a cyclic sieving phenomenon for sets of dissections of an n -gon using k diagonals. Our first main result (Theorem 1) is a cyclic sieving phenomenon on sets of dissections with a specified *type*, i.e., a list of the number of i -gons formed by the dissection for each $3 \leq i \leq n$. We suspect our polynomial is, up to

Key words and phrases. csp, polygons, frieze patterns, dissections, orbifolds.

powers of q , a refinement of the polynomial given in [RSW04, Theorem 7.1]. Dennis Stanton communicated a conjectural formula relating these polynomials; see Conjecture 1.

Our motivation for studying dissections of fixed type is partially due to the theory of frieze patterns. Outside of mathematics, a “frieze pattern” is a pattern in architecture or art with horizontal symmetry. It is classically known that there are seven types of symmetries a frieze can exhibit. Coxeter introduced a mathematical variant while studying Gauss’s Pentagramma mirificum [Cox71]. Together with Conway, they more fully established the theory of frieze patterns in two papers, one of which listed a set of questions [CC73a], while the second provided the solutions [CC73b]. Interest in frieze patterns has surged in the past 20 years since they were shown to have a connection to cluster algebras and representation theory [CC06]; see for instance [BFG⁺21, FP16, GHL23, Pro20].

The celebrated result in [CC73a, CC73b] is that there is a bijection between finite frieze patterns consisting of positive integers and triangulations of polygons (see Theorem 3). Holm and Jørgensen generalized this result by constructing a family of frieze patterns which are in 1-1 correspondence with p -angulations (i.e. dissections which cut a polygon into p -gons). These correspondences are useful as they link frieze patterns to a treasure trove of other mathematics (which we also exploit in Section 5). However, frieze patterns are defined to have infinite rows. From an enumerative standpoint, it would be more natural to count frieze patterns as living on a cylinder. That is, it would be more natural to count friezes up to a global shift of their rows. Understanding the cyclic sieving phenomenon on triangulations and more generally p -angulations allows us to do just that. This is stated in Proposition 7 and uses an alternate definition of the cyclic sieving phenomenon, stated in Proposition 6.

A triangulation of a polygon can have one of three types of rotational symmetry. Using a combinatorial interpretation of entries in a frieze pattern by Broline, Crowe, and Isaacs [BCI74], in Proposition 11, we characterize the associated frieze patterns in terms of *growth coefficients*, as in [BFPT19]. We then show that frieze patterns associated to triangulations with nontrivial rotational symmetry are in correspondence to homomorphisms on certain *finite-type (generalized) cluster algebras*; see Proposition 12 and Proposition 13. We remark that the former result follows directly from [FP16]. As these cluster algebras have geometric models via arcs on orbifolds, we refer to these as *frieze patterns from orbifolds*. [BK20, Proposition 4] implies that the frieze patterns considered here constitute all the finite, positive integral frieze patterns from orbifolds.

An *infinite frieze pattern* has one boundary row of 0’s and infinitely many rows extending in one direction. These also enjoy connections to cluster theory and representation theory [BQJ⁺24, BBG⁺24, GMV19, Pal22]. Baur, Parsons, and Tschabold gave a geometric model for infinite frieze patterns of positive integers [BPT16]. In particular, if the infinite frieze pattern has periodic rows, then it can be associated to a family of triangulated annuli or a family of triangulated once-punctured discs. The fact that this correspondence is not bijective makes enumeration less clear. By considering a cyclic-sieving phenomenon on once-punctured discs, using a q -analogue of a formula in [FP16], we enumerate certain families of infinite frieze patterns of integers (Theorem 9). We also extend the enumeration in [FP16] to $(m + 2)$ -angulations of a once-punctured polygon (Theorem 2) and find a partial cyclic sieving phenomenon in this setting (Proposition 10).

This narrative began with a Catalan object, namely, triangulations. *Dyck paths*, i.e. lattice paths from $(0, 0)$ to (n, n) which lie above the line $y = x$, are another well-studied and much loved Catalan object. Recently Cañadas, Gaviria, Rios, and Espinosa gave an explicit

connection between Dyck paths and finite, positive integral frieze patterns [CGRE23]. In [Proposition 15](#), we extend this latter construction to one between Holm-Jørgensen frieze patterns and p -Dyck paths, a common generalization. In line with the theme of the article, we also describe the induced map on Dyck paths and p -Dyck paths given by rotating the corresponding dissection; see [Theorem 10](#).

The remainder of this paper is split into four sections, which are organized as follows. We begin in [Section 2](#) by introducing notation that will be built upon in the later sections. This section also includes our cyclic sieving results on dissections of polygons. [Section 3](#) tells a parallel story in the context of dissections of punctured polygons. Unlike in the previous section, here some of the enumeration results are new. The results in these previous two sections are applied to frieze patterns in [Section 4](#), which also contains all necessary background information. All discussion involving Dyck paths is contained in [Section 5](#). Throughout the article, we have scattered questions and conjectures which we believe would lead towards interesting future work.

ACKNOWLEDGEMENTS

Ashleigh Adams was supported by NSF grant DMS-2247089 and NSF Graduate Fellowship Grant No. 2034612. We thank Vic Reiner and Dennis Stanton on enlightening conversations on the interactions between different cyclic sieving polynomials present in this topic. We would also like to thank Martin Rubey and Jessica Striker for helpful comments on earlier drafts. The second author thanks Emine Yıldırım for pointing out the reference [Pal08].

2. DISSECTIONS OF POLYGONS

In this section, we will exhibit a cyclic-sieving phenomenon on families of dissections ([Theorem 1](#)). We will also introduce notation that will be used in future sections.

Let P_n denote a polygon with n vertices. We will label these vertices v_0, v_1, \dots, v_{n-1} , traveling in clockwise order, and we will always treat these indices modulo n . A (counterclockwise) *rotation* of an n -gon, P_n , is a map on the vertices of P_n sending $v_i \mapsto v_{i-1}$ for all $0 \leq i \leq n-1$.

A *dissection* T of P_n is a set of non-crossing diagonals on P_n . We will refer to connected components of $P_n \setminus T$ as *subgons*, and we will refer to the number of vertices of a polygon as its *size*. Sometimes, we will conflate a dissection with this set of subgons. We say the *type* of a dissection T is a vector $(\mu_1(T), \dots, \mu_{n-2}(T))$ such that the number of $(i+2)$ -gons in $P_n \setminus T$ is $\mu_i(T)$. When the type $\mu(T)$ of T satisfies $\mu_i(T) = 0$ for all $i \neq m$, we call T a $(m+2)$ -*angulation*.

We first discuss an enumeration of all dissections of the same type. Let $\mu = (\mu_1, \mu_2, \dots, \mu_n) \in \mathbb{Z}_{\geq 0}^n$. Throughout this section, we will set $k = \mu_1 + \mu_2 + \dots + \mu_n$ and $n = \mu_1 + 2\mu_2 + \dots + n\mu_n$. By construction, it is possible to dissect P_{n+2} into μ_i $(i+2)$ -gons with $k-1$ non-crossing diagonals. Call the set of all such dissections \mathcal{A}_μ and let $a_\mu := |\mathcal{A}_\mu|$. A formula for a_μ was given as part of an exercise in [GJ04]:

$$a_\mu = \frac{1}{n+1} \binom{n+k}{k} \binom{k}{\mu_1, \mu_2, \dots, \mu_n}.$$

The numbers a_μ were also discussed in [DR01, WR25, SW16]. Note that if μ has only one nonzero part, say μ_m , then necessarily $\frac{n}{m}$ is a positive integer. Set $\ell = \frac{n}{m}$. After some

manipulations, a_μ for such a μ can be seen to be a Fuss-Catalan number:

$$c_\ell^{(m)} := a_{(0, \dots, 0, \mu_m, 0, \dots, 0)} = \frac{1}{m\ell + 1} \binom{(m+1)\ell}{\ell}.$$

In particular, if only the first part of μ is nonzero, then we recover the Catalan number $c_n := c_n^{(1)}$ which enumerates the triangulations of P_{n+2} .

We set $a_\mu(q)$ to be the naive q -analogue of a_μ , namely,

$$a_\mu(q) = \frac{1}{[n+1]_q} \left[\begin{matrix} n+k \\ k \end{matrix} \right]_q \left[\begin{matrix} k \\ \mu_1, \mu_2, \dots, \mu_n \end{matrix} \right]_q.$$

We define $c_\ell^{(m)}(q)$ and $c_n(q)$ accordingly. We will show that $a_\mu(q)$ functions as the cyclic sieving polynomial for \mathcal{A}_μ . First, we compute the evaluation of $a_\mu(q)$ at appropriate roots of unity. Recall that we set ζ_n to be a primitive n -th root of unity.

Lemma 1. *Let $\mu = (\mu_1, \mu_2, \dots, \mu_n)$, $k = \sum_{i=1}^n \mu_i$, and $n = \sum_{i=1}^n i\mu_i$. Let d be a positive integer such that $d|(n+2)$*

(1) *If there is one index j such that $\mu_j \equiv 1 \pmod{d}$ and $\mu_i \equiv 0 \pmod{d}$ for all $i \neq j$, then*

$$a_\mu(\zeta_d) = \binom{\frac{n+2}{d} + \frac{k-1}{d} - 1}{\frac{k-1}{d}} \left(\left\lfloor \frac{\mu_1}{d} \right\rfloor, \left\lfloor \frac{\mu_2}{d} \right\rfloor, \dots, \left\lfloor \frac{\mu_n}{d} \right\rfloor \right).$$

(2) *If $d = 2$ and all μ_i are even, then*

$$a_\mu(\zeta_2) = a_\mu(-1) = \binom{\frac{n+k}{2}}{\frac{k}{2}} \left(\frac{\mu_1}{2}, \frac{\mu_2}{2}, \dots, \frac{\mu_n}{2} \right).$$

(3) *If μ does not satisfy the above conditions, then $a_\mu(\zeta_d) = 0$.*

Proof. A standard way to compute such evaluations is to use the following identity. If $g \equiv h \pmod{d}$, then

$$(1) \quad \lim_{q \rightarrow \zeta_d} \frac{[g]_q}{[h]_q} = \begin{cases} \frac{g}{h} & g \equiv 0 \pmod{d} \\ 1 & \text{otherwise.} \end{cases}.$$

Therefore, most of the work comes from counting the number of terms in the numerator and denominator which are equivalent to 0 modulo d . In the set up of Cases (1) and (2), these numbers are the same and the resulting expressions are clear.

We now move on to showing Case (3), separating the proof into three cases, with this same method in mind. If k is not equivalent to 0 or 1 modulo d , then we immediately see $\left[\begin{smallmatrix} n+k \\ k \end{smallmatrix} \right]_{\zeta_d} = 0$.

If $k \equiv 0 \pmod{d}$, then the only way for $\left[\begin{smallmatrix} n+k \\ \mu_1, \mu_2, \dots, \mu_n \end{smallmatrix} \right]_{\zeta_d}$ to be nonzero is if $\mu_i \equiv 0 \pmod{d}$ for all i . If $d = 2$, then we are in Case (2). If $d > 2$, then it is impossible to have $2 + \sum_{i=1}^n i\mu_i = 2 + n$ be 0 modulo d .

Similarly, if $k \equiv 1 \pmod{d}$, and μ does not satisfy the condition in the hypothesis of part 1, then $\left[\begin{smallmatrix} n+k \\ \mu_1, \mu_2, \dots, \mu_n \end{smallmatrix} \right]_{\zeta_d} = 0$. \square

We now show that, if $d|(n+2)$ and μ satisfies the conditions in Case 1 or 2 of [Lemma 1](#), then the number of fixed points of \mathcal{A}_μ under $\frac{n}{d}$ -fold rotation is equal to the evaluation $a_\mu(\zeta_d)$. We refer to such a dissection as one having *d-fold symmetry*. In particular, 2-fold symmetry is a synonym for central symmetry. When we are in Case 1, we show this by explaining a way to encode each fixed point, which will make the enumeration apparent. Our proof is inspired by that of [\[EF08, Proposition 3.6\]](#). By keeping track of specific sizes of subgons, our process can be made more explicit.

Proposition 1. *Let $\mu = (\mu_1, \mu_2, \dots, \mu_n)$, $k = \sum_{i=1}^n \mu_i$, and $n = \sum_{i=1}^n i\mu_i$. Let d be a positive integer such that $d|(n+2)$.*

(1) *If there is exactly one value μ_j such that $\mu_j \equiv 1 \pmod{d}$ and $\mu_i \equiv 0 \pmod{d}$ for all $i \neq j$, then the number of dissections in \mathcal{A}_μ with d -fold symmetry is*

$$\binom{\frac{n+2}{d} + \frac{k-1}{d} - 1}{\frac{k-1}{d}} \binom{\frac{k-1}{d}}{\lfloor \frac{\mu_1}{d} \rfloor, \lfloor \frac{\mu_2}{d} \rfloor, \dots, \lfloor \frac{\mu_n}{d} \rfloor}.$$

(2) *Let $d = 2$. If all μ_i are even, then the number of dissections in \mathcal{A}_μ with d -fold symmetry is*

$$\binom{\frac{n+k}{2}}{\frac{k}{2}} \binom{\frac{k}{2}}{\frac{\mu_1}{2}, \frac{\mu_2}{2}, \dots, \frac{\mu_n}{2}}.$$

(3) *If d and μ do not satisfy either of the above conditions, then the number of dissections in \mathcal{A}_μ fixed by d -fold rotation is 0.*

Proof. **Item (1)** Notice our binomial $\binom{\frac{n+2}{d} + \frac{k-1}{d} - 1}{\frac{k-1}{d}}$ is equal to the multichoose coefficient $\binom{\binom{n+2}{d}}{\binom{k-1}{d}}$. For shorthand, set $g = \frac{k-1}{d}$. The desired formula suggests that we should find a bijection between dissections in \mathcal{A}_μ with d -fold symmetry (call this set \mathcal{A}_μ^d) and length g lists of tuples $(a_1, e_1), (a_2, e_2), \dots, (a_g, e_g)$ with the a_i satisfying $0 \leq a_1 \leq a_2 \leq \dots \leq a_g \leq \frac{n+2}{d} - 1$ and where the e_i form a multiset of elements from $[n] := \{1, \dots, n\}$ with number i appearing with multiplicity $\lfloor \frac{\mu_i}{d} \rfloor$.

Given $S \in \mathcal{A}_\mu^d$, we see that S is determined by its appearance in a $\frac{2\pi n}{d}$ sector, say, on the vertices $v_0, v_1, \dots, v_{\frac{n+2}{d}-1}$. For the following, we will consider each diagonal oriented so that the center of P_{n+2} lies to its right. This gives us a well-defined notion of the “starting point” of a diagonal.

There are $g = \frac{k-1}{d}$ orbits of diagonals under this rotation. Each orbit contains a unique representative whose starting point is in $V^d := \{v_0, v_1, \dots, v_{\frac{n+2}{d}-1}\}$. Let $a_1 \leq a_2 \leq \dots \leq a_g$ be the indices of the starting points, listed in weakly increasing order. We will think of each value a_i associated with the corresponding diagonal with starting point at v_{a_i} . When there are multiple diagonals with the same starting point, we will label these in counterclockwise order, so that the one with larger index is closer to the boundary edge (v_{a_i}, v_{a_i+1}) . Now, let $e_i + 2$ be the size of the subgon lying to the left of the i -th diagonal. Here, by “to the left”, we are again using the reference of the orientation given to this diagonal. Since either $d > 2$ or $d = 2$ and there is an even number of diagonals, there will be one subgon, whose size is a multiple of d , which will never be detected by this process since it lies to the right of all arcs. It follows that the list $(a_1, e_1), \dots, (a_g, e_g)$ will satisfy the desired conditions.

We claim this map is bijective. We describe an inverse map recursively. That is, we describe how to build an element of \mathcal{A}_μ^d from such a list. The smallest case is $g = \frac{k-1}{d} = 0$, which is associated to the trivial dissection on an $(n+2)$ -gon.

Now, we look more generally at a list $(a_1, e_1), \dots, (a_g, e_g)$ where in the multiset $\{e_1, \dots, e_g\}$ the number $i+2$ appears with multiplicity $\lfloor \frac{\mu_i}{d} \rfloor$. The key step is showing that there exists at least one value i such that $a_i + e_i + 1 \leq a_{i+1}$, where we interpret $a_{g+1} = a_1 + \frac{n+2}{d}$. Now, suppose for sake of contradiction that, for all $1 \leq i \leq g$, $a_i + e_i + 1 > a_{i+1}$, or equivalently $a_i + e_i \geq a_{i+1}$. Since a_{g+1} is defined to be $a_1 + \frac{n+2}{d}$, we also have an inequality $a_g + e_g \geq a_1 + \frac{n+2}{d}$. If we sum all g such inequalities and reduce, we have

$$e_1 + \dots + e_{g-1} + e_g \geq \frac{n+2}{d}.$$

Recall j is the index such that $\mu_j \equiv 1 \pmod{d}$. Now, we view the sum of the e_i in another way, using our initial assumptions about the vector μ ,

$$\begin{aligned} \sum_{i=1}^g e_i &= \sum_{i=1}^n \left\lfloor \frac{\mu_i}{d} \right\rfloor i \\ &= \sum_{i \neq j} \frac{\mu_i}{d} i + \frac{j(\mu_j - 1)}{d} \\ &= \frac{1}{d} \sum_{i=1}^n \mu_i i - \frac{j}{d} \\ &= \frac{n+2}{d} - \frac{j}{d} < \frac{n+2}{d}. \end{aligned}$$

Therefore, assuming $a_i + e_i + 1 > a_{i+1}$ for all i led to a contradiction. Given a list $(a_1, e_1), \dots, (a_g, e_g)$, pick the smallest i such that $a_i + e_i < a_{i+1}$. If we remove the pair (a_i, e_i) , we get a smaller list which has an associated dissection S' in $\mathcal{A}_{\mu'}^d$, where μ' is the result of subtracting 1 from μ_{e_i} . Then, the dissection for the original list is the result of adding an $(e_i + 2)$ -gon onto S' at each boundary edge in the orbit of (v_{a_i}, v_{a_i+1}) .

Item (2) If the number of subgons in a dissection is even, then the number of arcs used in the dissection is odd. In order for such a dissection to be fixed by 2-fold rotation, one arc in the dissection must be fixed by the rotation. This arc must be of the form $(i, i + \frac{n}{2})$. Such an arc cuts our polygon into two $(\frac{n}{2} + 1)$ -gons. We see that the dissection is fixed if these two smaller subgons have the same dissection, so that the number of fixed points is $\frac{n}{2}a_{\frac{n}{2}}$ where $\frac{\mu}{2} := (\frac{\mu_1}{2}, \frac{\mu_2}{2}, \dots, \frac{\mu_n}{2})$. The claim follows by simplifying the expression $\frac{n}{2}a_{\frac{n}{2}}$.

Item (3) If $d > 2$, then a necessary condition for a dissection to have d -fold symmetry is for there to be a central (ℓd) -gon, implying that the number of (ℓd) -gons in the entire dissection is 1 modulo d and the number of all other sized subgons is 0 modulo d . If $d = 2$, then there must either be a central (2ℓ) -gon for $\ell > 1$ or a central diagonal. In all such cases, we see that one of the conditions of μ from (1) or (2) must be satisfied. \square

Combining [Lemma 1](#) and [Proposition 1](#) gives the following immediately.

Theorem 1. *The triple $(\mathcal{A}_\mu, G_{n+2}, a_\mu(q))$ exhibits the cyclic sieving phenomenon.*

2.1. Relationship to Previous Work. In [\[RSW04, Theorem 7.1\]](#), Reiner, Stanton, and White discussed cyclic sieving phenomenon on the set of all dissections of P_n which use k

diagonals. The number of such dissections is $f(n, k) = \frac{1}{n+k} \binom{n+k}{k+1} \binom{n-3}{k}$, and the polynomial used their result is the naive q -analogue of this formula, i.e.,

$$f(n, k; q) := \frac{1}{[n+k]_q} \left[\begin{array}{c} n+k \\ k+1 \end{array} \right]_q \left[\begin{array}{c} n-3 \\ k \end{array} \right]_q.$$

The sets \mathcal{A}_μ partition the cyclic orbits of dissections of P_{n+2} using $k-1$ diagonals since the size of subgons in a dissection do not change under rotation. So it is natural to expect a relation between $f(n+2, k-1; q)$ and the family of polynomials $a_\mu(q)$ with $k = \sum_{i=1}^n \mu_i$ and $n = \sum_{i=1}^n i\mu_i$. Such a relationship was conjectured to us by Dennis Stanton [Sta].

Notice each μ encodes a partition $\lambda(\mu) = (\lambda_1, \dots, \lambda_k)$ of n into k parts, where μ_i is the number of parts of λ of size i . Write $\lambda(\mu) = (\lambda_1 > \lambda_2 > \dots > \lambda_k)$ in decreasing order and then set

$$b(\mu) := 2k\lambda_1 + 2(k-1)\lambda_2 + \dots + 2\lambda_{k-1} + \lambda_k.$$

Conjecture 1 (Stanton's Conjecture). *The polynomials $f(n, k; q)$ and $a_\mu(q)$ are related by*

$$q^{2n+k(k-1)} f(n+2, k-1; q) = \sum_{\mu} q^{b(\mu)} a_\mu(q)$$

where the righthand side is a sum over all $\mu \in \mathbb{Z}_{\geq 0}^n$ satisfying $\sum_{i=1}^n \mu_i = k$ and $\sum_{i=1}^n i\mu_i = n$.

After some algebraic manipulations, one can see that Conjecture 1 can be simplified as

$$(2) \quad q^{2n+k(k-1)} \left[\begin{array}{c} n-1 \\ k-1 \end{array} \right]_q = \sum_{\mu} q^{b(\mu)} \left[\begin{array}{c} k \\ \mu_1, \dots, \mu_n \end{array} \right]_q.$$

Note that at $q = 1$, Equation (2) recovers a simple formula regarding the number of weak compositions of n .

When $k = 2$, verifying Equation (2) is quite easy. We were able to inductively verify Equation (2) for $k = 3$ using the following process. Let the set of partitions of n into k parts be denoted $P(n, k)$. There is a natural inclusion, call it ι , from $P(n-1, k)$ into $P(n, k)$ given by $\iota(\lambda_1, \dots, \lambda_k) = (\lambda_1 + 1, \dots, \lambda_k)$. When $k = 3$, one can characterize the complement $P(n, 3) \setminus \iota(P(n-1, 3))$ as well as all $\lambda \in P(n-1, 3)$ such that the number of distinct parts in λ differs from the number in $\iota(\lambda)$. Using these observations, we can classify the difference of the right-hand side of Equation (2) for $k = 3$ and the pair $n-1, n$ and show it matches the difference of the left-hand side.

Eu and Fu generalized [RSW04, Theorem 7.1] to *s-divisible dissections*. These are dissections in which every subgon has size $sj+2$ for a fixed positive integer s ; the setting of Reiner, Stanton and White's work is the $s = 1$ case. Dissections into $(sj+2)$ -gons form a geometric model of the faces of a generalized cluster complex in type A [FR05].

Note that s -divisible dissections only exist for polygons with $sn+2$ vertices. The polynomial which Eu and Fu associated to the set of s -divisible dissections of P_{sn+2} with k diagonals is

$$G(s, n, k; q) = \frac{1}{[sn+k+2]_q} \left[\begin{array}{c} sn+k+2 \\ k+1 \end{array} \right]_q \left[\begin{array}{c} n-1 \\ k \end{array} \right]_q.$$

Based on Conjecture 1, one would hope that $G(s, n, k; q)$ can also be written as a sum of polynomials $a_\mu(q)$, multiplied by appropriate q -powers.

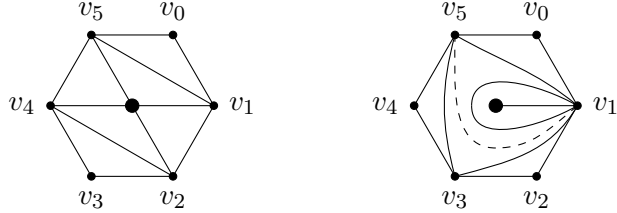


FIGURE 1. Two triangulations of P_6^\bullet . Arc (v_1, v_5) in the triangulation on the right is dashed for emphasis.

Question 1. Fix positive integers s and n and let $1 \leq k \leq n$. Is there a family of integers $b_s(\mu)$ such that

$$G(s, n, k - 1; q) = \sum_{\mu} q^{b_s(\mu)} a_{\mu}(q)$$

where the righthand side is a sum over all $\mu \in \mathbb{Z}_{\geq 0}^{sn+2}$ satisfying $\sum_{i=1}^n \mu_i = k$, $\sum_{i=1}^n i \mu_i = sn$, and $\mu_i > 0$ only if s divides $i + 2$?

3. $(m + 2)$ -ANGULATIONS OF PUNCTURED POLYGONS

Let P_n^\bullet denote a disc with n marked points on the boundary and one on the interior, referred to as a (once) punctured polygon. As before, we will enumerate the vertices on the boundary as v_0, \dots, v_{n-1} moving clockwise. We will refer to the marked point on the interior, i.e. the puncture, as \bullet .

We will refer to non-self-intersecting curves with endpoints in marked points $\{v_0, \dots, v_{n-1}, \bullet\}$ as *arcs* and we will refer to maximal sets of pairwise non-crossing arcs as *triangulations*. We remark that arcs are always considered up to isotopy and so saying a pair of arcs does not cross precisely means there exist non-crossing representatives in the isotopy class of each.

Arcs incident to the puncture, i.e. those of the form (v_i, \bullet) , will be referred to as *spokes*. For example, consider the two triangulations of P_6^\bullet in Figure 1. The triangulation on the left has four spokes while the triangulation on the right has one spoke. By the maximality of a triangulation, every triangulation of P_n^\bullet will have at least one spoke.

Given $i \neq j$, there are two non-isotopic arcs incident to v_i and v_j . Notice every arc separates P_n^\bullet into a smaller (ordinary) polygon and a smaller punctured polygon. We let (v_i, v_j) be the arc such that the vertices v_{i+1}, \dots, v_{j-1} sit in the smaller polygon without a puncture. For example, in Figure 1, both triangulations have the arc (v_5, v_1) , but only the triangulation on the right contains the arc (v_1, v_5) . We have dashed (v_1, v_5) in the triangulation on the right for emphasis.

There are two special instances of arcs between boundary vertices. The boundary edges are exactly (v_i, v_{i+1}) . For each $0 \leq i \leq n - 1$, we also have the arc (v_i, v_i) which cuts out a once-punctured monogon. For instance, the triangulation on the right in Figure 1 contains the arcs (v_1, v_1) .

Definition 2. Let $m \geq 1$. An $(m + 2)$ -angulation T on P_n^\bullet is a set of arcs which are pairwise non-crossing and such that all connected components of $P_n^\bullet \setminus T$ are $(m + 2)$ -gons.

The latter condition implies that every $(m + 2)$ -angulation contains at least one spoke since otherwise there would be a connected component which contained the puncture.

3.1. Enumeration. Our goal in this section is to enumerate all $(m + 2)$ -angulations of P_n^\bullet with a fixed number of spokes. First, we determine the necessary relationship between n and m in order for $(m + 2)$ -angulations of P_n^\bullet to exist.

Lemma 2. *An $(m + 2)$ -angulation of P_n^\bullet exists if and only if $n = m\ell$ for $\ell \geq 1$. If $n = m\ell$, there are exactly ℓ connected components in $P_n^\bullet \setminus T$ for every $(m + 2)$ -angulation T .*

Proof. Every $(m + 2)$ -angulation must have at least one spoke. Given such a spoke, say (v_i, \bullet) , we see that the $P_n - (v_i, \bullet)$ is a $(n + 2)$ -gon. It is well-known that an $(m + 2)$ -angulation of P_{n+2} exists exactly when $n + 2 = m\ell + 2$ for some $\ell \geq 1$, and such an $(m + 2)$ -angulation breaks P_{n+2} into ℓ total $(m + 2)$ -gons. \square

Fontaine and Plamondon [FP16] enumerated triangulations of P_n^\bullet with a fixed number of spokes. Our enumeration is inspired by theirs and in particular we recover their enumeration in the triangulation case. Fontaine and Plamondon's proof used the fact that the number of triangulations of P_n which do not include any diagonals incident to a fixed vertex is a Catalan number. As an intermediate result, we provide a computation for the analogous situation, but instead for $(m + 2)$ -angulations. To that end, define $p_\ell^{(m)}$ to be the number of $(m + 2)$ -angulations of $P_{m\ell+2}$ which do not include a diagonal of the form (v_0, v_i) for any $2 \leq i \leq m\ell$.

In the following, let $c^{(m)}(x) = \sum_{\ell \geq 0} c_\ell^{(m)} x^\ell$ be the generating function of the Fuss-Catalan numbers. Recall $c_\ell^{(m)} = \frac{1}{m\ell+1} \binom{(m+1)\ell}{\ell}$ counts the number of $(m + 2)$ -angulations of a $P_{m\ell+2}$.

Lemma 3. *The generating function for the numbers $p_\ell^{(m)}$ is given by*

$$p^{(m)}(x) := \sum_{\ell \geq 0} p_\ell^{(m)} x^\ell = x c^{(m)}(x)^m.$$

Proof. Set $n = m\ell + 2$. An $(m + 2)$ -angulation of P_n breaks the polygon into ℓ subgons. If an $(m + 2)$ -angulation does not include any diagonals incident to v_0 , then v_0 lies on a unique $(m + 2)$ -gon, say Q , and v_1 and v_{n-1} also lie on Q . That is, (v_{n-1}, v_0) and (v_0, v_1) are edges of Q .

The subgon Q will have m additional edges. These must be placed so that the resulting subgons can be $(m + 2)$ -angulated. We can see the number of ways to do this as the number of ways to write $\ell - 1$ as a sum of m nonnegative integers, where each integer counts the number of subgons needed to $(m + 2)$ -angulate the subgon cut out by one edge of Q . In particular, we have a contribution of 0 when an edge of Q coincides with an edge in P_n .

Given an admissible choice of edges for Q , yielding the weak composition $i_1 + i_2 + \dots + i_m = \ell - 1$, we see the number of ways to complete this to an $(m + 2)$ -angulation of P_n is $c_{i_1}^{(m)} c_{i_2}^{(m)} \dots c_{i_m}^{(m)}$. By considering all possible choices of i_1, i_2, \dots, i_m , we have

$$p_\ell^{(m)} = \sum_{i_1 + \dots + i_m = \ell - 1} c_{i_1}^{(m)} c_{i_2}^{(m)} \dots c_{i_m}^{(m)} = [x^{\ell-1}] c^{(m)}(x)^m.$$

The claim now follows. \square

Understanding the quantity $p_\ell^{(m)}$ in terms of Fuss-Catalan numbers enables us to do the desired enumeration.

Theorem 2. *Let $n = m\ell$ and let $1 \leq s \leq \ell$. The number of $(m+2)$ -angulations of P_n^\bullet with s spokes is $m \binom{n+\ell-s-1}{n-1}$.*

Proof. It is easiest to first only consider $(m+2)$ -angulations of P_n^\bullet which include the spoke (v_0, \bullet) . We must choose $s-1$ additional spokes in such a way that the polygons cut out by consecutive spokes can be $(m+2)$ -angulated. Recall from Lemma 2 that any $(m+2)$ -angulation of P_n^\bullet will contain ℓ subgons. We can see our choices of valid locations for spokes as a way to write ℓ as a sum of s positive integers, i.e., a composition of ℓ . In particular, the composition, say $j_1 + \dots + j_s = \ell$ is associated to a choice of spokes such that connected component cut out by the first spoke (i.e. (v_0, \bullet)) and second is a polygon of size $m j_1 + 2$, and so on. For one such admissible set of spokes, we then put an $(m+2)$ -angulation on each smaller polygon. When doing this, we do not want to include any diagonal incident to \bullet since we have already chosen all of our spokes. Therefore, we see that the number of ways to complete this choice to an $(m+2)$ -angulation is $p_{j_1}^{(m)} p_{j_2}^{(m)} \dots p_{j_s}^{(m)}$. Then, if we sum all possible choices of spokes, we have

$$\sum_{j_1 + \dots + j_s = \ell} p_{j_1}^{(m)} p_{j_2}^{(m)} \dots p_{j_s}^{(m)} = [x^\ell] (p^{(m)}(x))^s = [x^{\ell-s}] (c^{(m)}(x))^{ms}$$

where the last equality follows from Lemma 3. Note that since $p^{(m)}(x)$ has no constant term, summing over compositions here is equivalent to summing over weak compositions.

From [GKP94, Equation 7.70]¹, we have that

$$\begin{aligned} [x^{\ell-s}] (c^{(m)}(x))^{ms} &= \frac{ms}{(\ell-s)(m+1)+ms} \binom{(\ell-s)(m+1)+ms}{\ell-s} \\ &= \frac{ms}{n+\ell-s} \binom{n+\ell-s}{n} \end{aligned}$$

where the second equality follows from substituting $\ell m = n$.

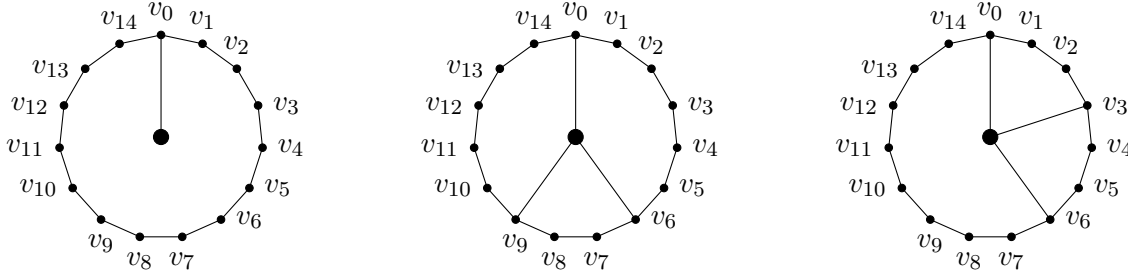
So far, we have enumerated all $(m+2)$ -angulations of P_n^\bullet with s spokes where one spoke is (v_0, \bullet) . We will encounter every $(m+2)$ -angulation with s spokes by rotating each such dissection with a spoke (v_0, \bullet) n times (including the trivial rotation). Doing this in fact produces every $(m+2)$ -angulation s times as each spoke will be incident to v_0 at one rotation. Therefore, the total number of $(m+2)$ -angulations of P_n^\bullet with s spokes is

$$\frac{n}{s} \cdot \frac{ms}{n+\ell-s} \binom{n+\ell-s}{n} = m \binom{n+\ell-s-1}{n-1}.$$

□

Example 1. Here, we illustrate how to enumerate 5-angulations of P_{15}^\bullet with 3 spokes.

¹Note that our choice of index on the Fuss-Catalan numbers differs from the convention in this reference.



Since $15 = 3 \cdot 5$, when we begin with a spoke (v_0, \bullet) , the admissible ways to add two more spokes correspond with the compositions of 5 with 3 parts. These are $2 + 2 + 1, 2 + 1 + 2, 1 + 2 + 2, 3 + 1 + 1, 1 + 3 + 1$ and $1 + 1 + 3$. For example, the composition $2 + 1 + 2$ corresponds to placing spokes (v_6, \bullet) and (v_9, \bullet) , as in the middle above, while the composition $1 + 1 + 3$ corresponds to placing spokes (v_3, \bullet) and (v_6, \bullet) , as on the right above.

There are $(p_2^{(5)})^2 p_1^{(5)} = 9$ ways to complete the middle picture to a 5-angulation without adding more spokes and similarly there are $p_3^{(5)}(p_1^{(5)})^2 = 15$ ways to complete the right picture to a 5-angulation with 3 spokes. As prescribed in the proof of [Theorem 2](#), we see there are $27 + 45 = 72$ total 5-angulations of P_{15}^\bullet with 3 spokes which include (v_0, \bullet) , and overall there are 360 total 5-angulations of P_{15}^\bullet .

Corollary 1. *Let $n = m\ell$ for $m, \ell \geq 1$. The number of $(m + 2)$ -angulations of P_n^\bullet is $m \binom{n+\ell-1}{n} = \binom{n+\ell-1}{\ell}$.*

Proof. The number of spokes in an $(m + 2)$ -angulation of P_n^\bullet is at least 1 and at most ℓ . We reach our first expression by summing the number of $(m + 2)$ -angulations with each number of spokes, using [Theorem 2](#) and applying the “Hockey-Stick identity,” $\sum_{i=a}^b \binom{i}{a} = \binom{b+1}{a+1}$. The second expression follows from a few algebraic manipulations. \square

3.2. Cyclic Sieving. Here, we will show that the natural q -analogue of our counting formula in [Theorem 2](#) often works as a cyclic sieving polynomial for the set of $(m + 2)$ -angulations of P_n^\bullet .

To this end, let $\mathcal{T}_{n,s}^{\bullet, (m)}$ denote the set of $(m + 2)$ -angulations of P_n^\bullet with s spokes. Naturally, $\mathcal{T}_{n,s}^{\bullet, (m)}$ is only nonempty if m divides n and $1 \leq s \leq \frac{n}{m}$. Given such a value s , define $t_{n,s}^{(m)} = m \binom{n+\frac{n}{m}-s-1}{n-1}$ so that $t_{n,s}^{(m)}$ is the cardinality of $\mathcal{T}_{n,s}^{\bullet, (m)}$. We also define

$$t_{n,s}^{(m)}(q) := m \left[\begin{array}{c} n + \frac{n}{m} - s - 1 \\ n - 1 \end{array} \right]_q.$$

The group $G_n = \langle \sigma \rangle$ of rotations defined in [Section 2](#) also acts naturally on $\mathcal{T}_{n,s}^{\bullet, (m)}$. Our goal now is to show that the polynomial $t_{n,s}^{(m)}(q)$ functions as a cyclic sieving polynomial for many n -th roots of unity. The proof of [Proposition 2](#) will use the following computations.

Lemma 4. *Let d, k , and n be positive integers.*

- (1) *If $n \equiv k \pmod{d}$, then $\left[\begin{smallmatrix} n \\ k \end{smallmatrix} \right]_{q=\zeta_d} = \binom{\lfloor \frac{n}{d} \rfloor}{\lfloor \frac{k}{d} \rfloor}$.*
- (2) *If $k \equiv -1 \pmod{d}$ and $n \not\equiv -1 \pmod{d}$, then $\left[\begin{smallmatrix} n \\ k \end{smallmatrix} \right]_{q=\zeta_d} = 0$.*

Proof. Each statement can be shown using Equation (1). For instance, in Case (1), we have

$$\lim_{q \rightarrow \zeta_d} \left[\begin{matrix} n \\ k \end{matrix} \right]_q = \frac{(\lfloor \frac{n}{d} \rfloor)(\lfloor \frac{n}{d} \rfloor - 1) \cdots (\lfloor \frac{n}{d} \rfloor - \lfloor \frac{k}{d} \rfloor + 1)}{(\lfloor \frac{k}{d} \rfloor)(\lfloor \frac{k}{d} \rfloor - 1) \cdots 1} = \binom{\lfloor \frac{n}{d} \rfloor}{\lfloor \frac{k}{d} \rfloor},$$

immediately seeing the desired conclusion. Similarly, Case (2) can be shown by observing that there are more factors of the minimal polynomial of ζ_d in the numerator than in the denominator of the expression

$$\frac{[n][n-1] \cdots [n-k+1]}{[k][k-1] \cdots [1]}.$$

□

Proposition 2. *Let m and ℓ be two positive integers and set $n = m\ell$. Let $1 \leq s \leq \ell$, and let d be a divisor of n . If s and ℓ are not equivalent to the same nonzero number mod d , then $t_{n,s}^{(m)}(\zeta_d)$ is equal to the number of $(m+2)$ -angulations in $\mathcal{T}_{n,s}^{\bullet,(m)}$ which are fixed by $\sigma^{\frac{n}{d}}$.*

Proof. Let $d|n$. Let T be an $(m+2)$ -angulation in $\mathcal{T}_{n,s}^{\bullet,(m)}$ which is fixed by $\sigma^{\frac{n}{d}}$. In order for T to exist, we need $d|s$ and $d|\ell$. The latter condition is necessary when we remember from Lemma 2 that ℓ counts the number of $(m+2)$ -gons cut out by any element of $\mathcal{T}_{n,s}^{\bullet,(m)}$.

Since T is fixed by $\sigma^{\frac{n}{d}}$, it is completely determined by any $2\pi/d$ sector, such as $v_0, v_1, \dots, v_{\frac{n}{d}-1}$. If we cut out the sector formed by $v_0, \dots, v_{\frac{n}{d}-1}, v_{\frac{n}{d}}$ and identifying v_0 and $v_{\frac{n}{d}}$, we have an element of $\mathcal{T}_{\frac{n}{d},\frac{s}{d}}^{\bullet,(m)}$. This process in fact gives a bijection between the elements of $\mathcal{T}_{n,s}^{\bullet,(m)}$ fixed by $\sigma^{\frac{n}{d}}$ and $\mathcal{T}_{\frac{n}{d},\frac{s}{d}}^{\bullet,(m)}$. Therefore, the number of fixed points of $\sigma^{\frac{n}{d}}$ in $\mathcal{T}_{n,s}^{\bullet,(m)}$ is exactly $t_{\frac{n}{d},\frac{s}{d}}^{(m)} = m\left(\frac{n}{d} + \frac{\ell}{d} - \frac{s}{d} - 1\right)$.

Now, we turn to evaluating $t_{n,s}^{(m)}(q)$ at $q = \zeta_d^{\frac{n}{d}}$, or equivalently, ζ_d . First, suppose we have $d|s$ and $d|\ell$, so that there are d -fixed points in $\mathcal{T}_{n,s}^{\bullet,(m)}$. Then, since $n + \ell - s - 1 \equiv n - 1 \pmod{d}$, we can use Lemma 4 to show

$$t_{n,s}^{(m)}(\zeta_d) = \left[\begin{matrix} n + \ell - s - 1 \\ n - 1 \end{matrix} \right]_{q=\zeta_d} = \binom{\lfloor \frac{n+\ell-s-1}{d} \rfloor}{\lfloor \frac{n-1}{d} \rfloor} = \binom{\frac{n}{d} + \frac{\ell}{d} - \frac{s}{d} - 1}{\frac{n}{d} - 1},$$

as desired.

Suppose now that at least one of ℓ or s is not equivalent to 0 modulo d . Moreover, assume $\ell \not\equiv s \pmod{d}$, which implies $n + \ell - s - 1 \not\equiv -1 \pmod{d}$. Since $n - 1 \equiv -1 \pmod{d}$, by Lemma 4, $t_{n,s}^{(m)}(\zeta_d) = 0$. □

Let $t_n(q) = \sum_{s=1}^n t_{n,s}^{(1)}(q)$. By Corollary 1, $t_n(q)$ is a q -analogue of $\binom{2n-1}{n}$. Let \mathcal{T}_n^\bullet denote the set of all triangulations of P_n^\bullet . Note that if $m = 1$, the ℓ in the statement of Proposition 2 is equal to n and thus will never be equivalent to a nonzero number modulo d , a divisor of n . Thus, the following is immediate.

Proposition 3. *The triple $(\mathcal{T}_n^\bullet, G_n, t_n(q))$ exhibits the cyclic sieving phenomenon.*

Remark 1. Proposition 3 bears similarity to the work of Eu and Fu [EF08] who exhibited cyclic sieving phenomena for generalized cluster complexes. This is similar because triangulations of P_n^\bullet model clusters in a type D cluster algebra and hence these will correspond to facets of the (ordinary) cluster complex. We note that Eu and Fu use instead a model given in [FZ03]

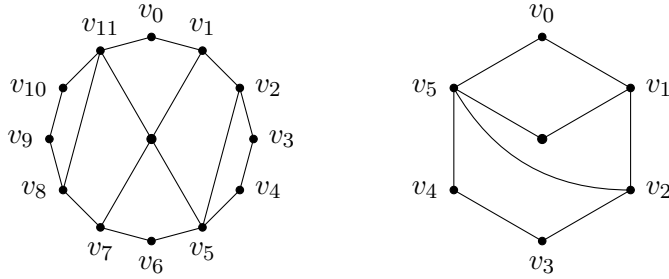


FIGURE 2. Associating a smaller 4-angulation to a 4-angulation with 2-fold symmetry, as in the proof of Proposition 2.

which uses colored diagonals on an ordinary polygon. Our result is not a special case of that in [EF08] as the cyclic actions differ. In particular, the action in Eu and Fu's work, which resembles Auslander-Reiten translation, has order \$2n\$ when \$n\$ is odd whereas our action is always order \$n\$.

When \$s \equiv \ell \pmod{d}\$ and these are not divisible by \$d\$, then \$t_{n,s}^{(m)}(\zeta_d) \neq 0\$ even though there are no triangulations fixed by \$\sigma^{\frac{n}{d}}\$ in \$\mathcal{T}_{n,s}^{\bullet, (m)}\$. It is not clear what \$t_{n,s}^{(m)}(\zeta_d)\$ counts in this case. For example, given if \$n = 12\$ and \$m = 3\$, implying \$\ell = 4\$, and \$s = 1\$, then we have \$t_{12,1}^{(3)}(\zeta_3) = 3 \left[\begin{smallmatrix} 14 \\ 11 \end{smallmatrix} \right]_{q=\zeta_3} = 3 \binom{4}{3} = 12\$. Meanwhile, \$\mathcal{T}_{12,1}^{\bullet, (3)}\$ consists of 5-angulations of \$P_{12}^{\bullet}\$ with one spoke, and such 5-angulations never have nontrivial rotational symmetry. Therefore, for general \$m\$, our analogue of Proposition 2 must avoid such behavior.

Proposition 4. *Let \$n, m\$, and \$s\$ be three positive integers such that \$m\$ divides \$n\$ and for all divisors \$d\$ of \$n\$, if \$s \equiv \frac{n}{m} \pmod{d}\$, then \$s \equiv 0 \pmod{d}\$. The triple \$(\mathcal{T}_{n,s}^{\bullet, (m)}, G_n, t_{n,s}^{(m)})\$ exhibits the cyclic sieving phenomenon.*

An example of a triple of positive integers satisfying the conditions of Proposition 4 is \$n = 12, m = 3, s = 3\$.

Question 2. *Given \$n = m\ell\$, \$d\$ a divisor of \$n\$, and \$1 \leq s \leq \ell\$ such that \$s \equiv \ell \not\equiv 0 \pmod{d}\$, is there a natural subset of \$\mathcal{T}_{n,s}^{\bullet, (m)}\$ with cardinality \$t_{n,s}^{(m)}(\zeta_d)\$?*

4. FRIEZE PATTERNS

We now seek to apply our cyclic sieving results to frieze patterns, combinatorial objects with connections to cluster theory, representation theory, and geometry. Several lovely surveys about frieze patterns have been recently written, such as [Bau21, MG15, Pre23].

Definition 3. *A frieze pattern of width \$n\$ over an integral domain \$R\$ is a function \$F : \{(i, j) \in \mathbb{Z} \times \mathbb{Z} : 0 \leq i - j \leq n\} \rightarrow R\$ satisfying*

- (1) \$F(i, i) = F(i, n+i) = 0\$ and \$F(i, i+1) = F(i, n+i-1) = 1\$ for all \$i \in \mathbb{Z}\$, and
- (2) for all \$i \leq j\$, \$F(i-1, j)F(i, j+1) - F(i, j)F(i+1, j+1) = 1\$.

An infinite frieze pattern over a ring \$R\$ is a function \$F : \{(i, j) \in \mathbb{Z} \times \mathbb{Z} : 0 \leq i - j\} \rightarrow R\$ satisfying

- (1') \$F(i, i) = 0\$ and \$F(i, i+1) = 1\$ for all \$i \in \mathbb{Z}\$, and
- (2) for all \$i \leq j\$, \$F(i-1, j)F(i, j+1) - F(i, j)F(i+1, j+1) = 1\$.

We remark that width n frieze patterns here would often be referred to as having width $n - 3$ in other articles.

The values of the frieze pattern are usually depicted as an array with every other row shifted as below, and we will conflate the data of F with such arrays. When drawn this way, condition in (2) becomes the rule that, in every diamond, the product of the horizontal entries is one more than the product of the vertical (most simply, East \times West - North \times South = 1). Note that in this depiction, the rows are of the form $(F(i, i + k))_{i \in \mathbb{Z}}$ for a fixed value k .

$$\begin{array}{ccccccc}
 \dots & 0 & & 0 & & 0 & \dots \\
 & & 1 & & 1 & & \dots \\
 \dots & F(-1, 1) & F(0, 2) & F(1, 3) & F(2, 4) & F(3, 5) & \dots \\
 \dots & F(-1, 2) & F(0, 3) & F(1, 4) & F(2, 5) & & \dots \\
 \dots & F(-2, 2) & F(-1, 3) & F(0, 4) & F(1, 5) & F(2, 6) & \dots \\
 \dots & F(-2, 3) & F(-1, 4) & F(0, 5) & F(1, 6) & & \dots \\
 & \ddots & & \vdots & & \ddots & \\
 \end{array}$$

For explicit examples of a frieze pattern, see [Example 2](#) and [Example 3](#).

We introduce more terminology associated to frieze patterns. These apply to both finite frieze patterns (i.e. frieze patterns with a positive integral width) and infinite frieze patterns. In this article, all infinite frieze patterns will be assumed to be *periodic*, i.e. each row will be periodic.

Definition 4. Let F be a frieze pattern over a ring R .

- (1) The row $(F(i, i + 2))$ is called the quiddity row.
- (2) If all 3×3 diamonds in F form a matrix with determinant 0, we say F is tame.

One can check that all examples of frieze patterns provided here are tame.

The unimodular rule (i.e. part (2) of [Definition 3](#)) implies that a frieze pattern is determined by its quiddity row. Indeed, the relationship between any value of a frieze pattern and the quiddity row can be made explicit. Define a family of multivariate polynomials $K_n(x_1, \dots, x_n)$ by $K_0 = 1$ and $K_n(x_1, \dots, x_n) = x_n K_{n-1}(x_1, \dots, x_{n-1}) + K_{n-2}(x_1, \dots, x_{n-2})$. The polynomials $K_n(\mathbf{x})$ are known as *continuants* and can also be defined as a determinant of a tridiagonal matrix. The following comes from [\[CC73a, CC73b, Question 18\]](#).

Lemma 5. Given a frieze pattern F and integers $i < j$,

$$F(i, j) = K_{j-i-1}(F(i, i + 2), F(i + 1, i + 3), \dots, F(j - 2, j)).$$

4.1. Frieze Patterns from Dissections. Frieze patterns were introduced by Coxeter in [\[Cox71\]](#). Shortly after their first appearance, Conway and Coxeter characterized finite frieze patterns over \mathbb{Z} with positive entries, i.e. positive integral frieze patterns [\[CC73a, CC73b\]](#). Holm and Jørgensen generalized this result to $(m + 2)$ -angulations [\[HJ20\]](#). We first define frieze patterns associated to any dissection of a polygon and then refine to these cases. Given p a positive integer, set $\lambda_p := 2 \cos(\pi/p)$. Let \bar{i} denote i modulo n .

Definition 5. Let T be a dissection of P_{n+3} . For each vertex v_j and all $p \geq 3$, let $\mu_p(j)$ denote the number of p -gons of T incident to v_j . We define F_T , the frieze pattern associated to T , to be the frieze pattern with quiddity row given by setting $F(i - 1, i + 1) = \sum_{p \geq 3} \mu_p(i) \lambda_p$.

See [Example 2](#) for two frieze patterns associated to dissections. This construction is an extension of the classical bijection between positive integral frieze patterns and triangulations of polygons.

Theorem 3 ([CC73a, CC73b]). *Every positive integral frieze pattern of width n is uniquely associated to a triangulation of P_n .*

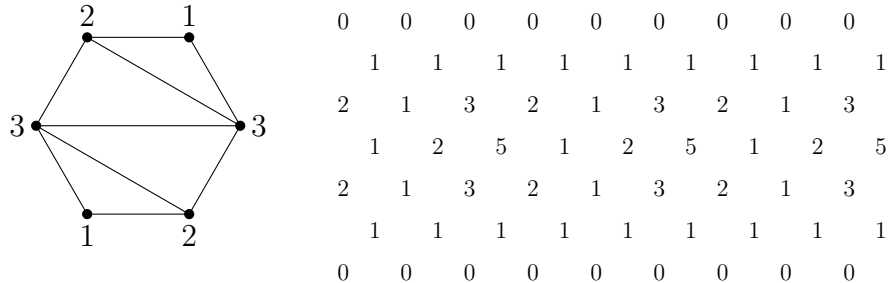
Holm and Jørgensen give a parallel theorem for general $(m+2)$ -angulations. The corresponding frieze patterns are said to be of *type Λ_{m+2}* . A frieze pattern is of type Λ_{m+2} if its quiddity row consists of positive integral multiples of λ_{m+2} .

Theorem 4 ([HJ20]). *Every frieze pattern of type Λ_{m+2} and width n is uniquely associated to an $(m+2)$ -angulation of P_n .*

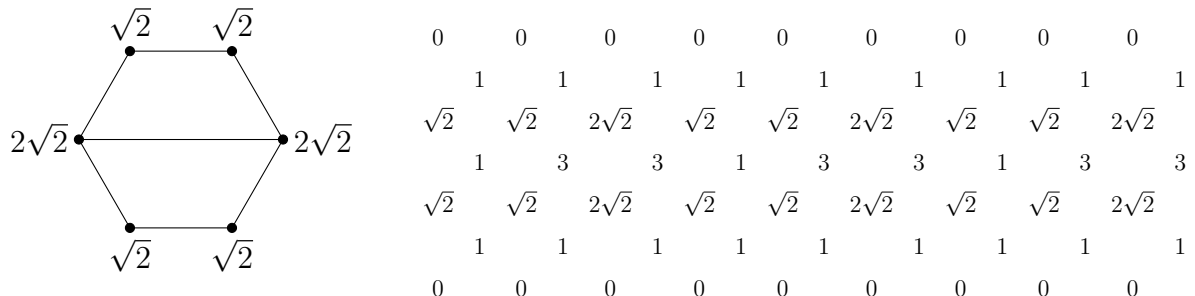
No similar characterization of frieze patterns from general dissections is known. However, Holm and Jørgensen showed that these always the expected width.

Proposition 5 ([HJ20]). *If F_T is a frieze pattern associated to a dissection T of P_n , then F_T has width n .*

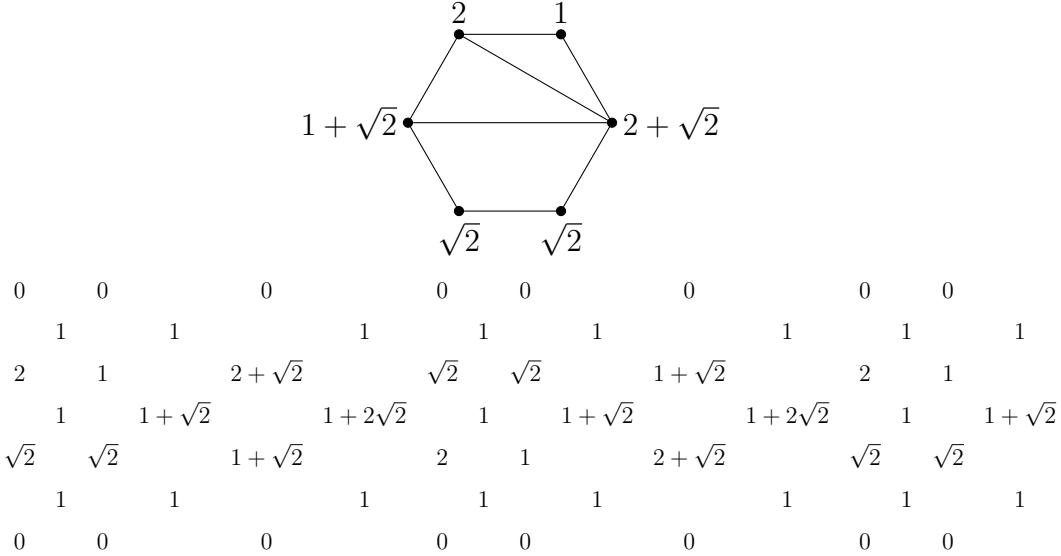
Example 2. First, we illustrate [Theorem 3](#) by giving an example of a triangulated hexagon and the corresponding frieze pattern with width 3. We label each vertex v_i with $F(i-1, i+1)$.



Now, we turn to the setting of [Theorem 4](#). Consider the 4-angulation of a hexagon below. The associated frieze pattern still has width 3 but it now has values in $\mathbb{Z}[\sqrt{2}]$ since $\lambda_4 = \sqrt{2}$.



Finally, we consider a dissection of a hexagon which consists of subgons of different sizes.



[Theorem 3](#) and [Theorem 4](#) have immediate, enumerative corollaries.

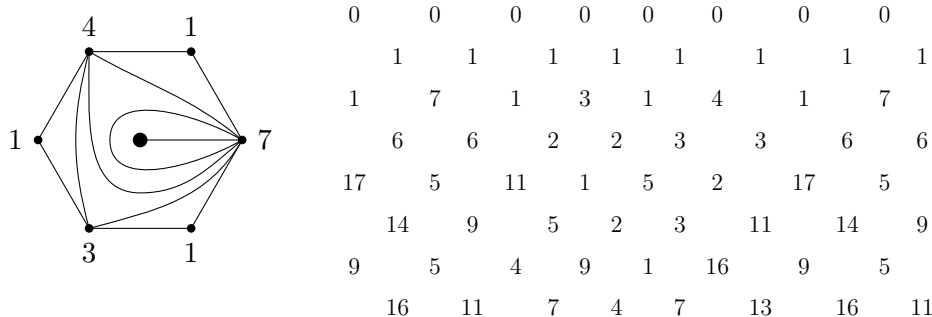
Corollary 2. *Frieze patterns of type Λ_{m+2} and width n only exist if $n = m\ell + 2$. If $n = m\ell + 2$, then there are $c_\ell^{(m)}$ frieze patterns of type Λ_{m+2} and width n . In particular, there are c_{n-2} positive integral frieze patterns of width n .*

To discuss a geometric model for infinite frieze patterns, we will need to extend [Definition 5](#). Let S be an arbitrary orientable surface with nonempty boundary and a finite set of marked points. Assume moreover that every boundary component of S contains at least one marked point. A dissection T of S is said to be *cellular* if all connected components in $S \setminus T$ are discs.

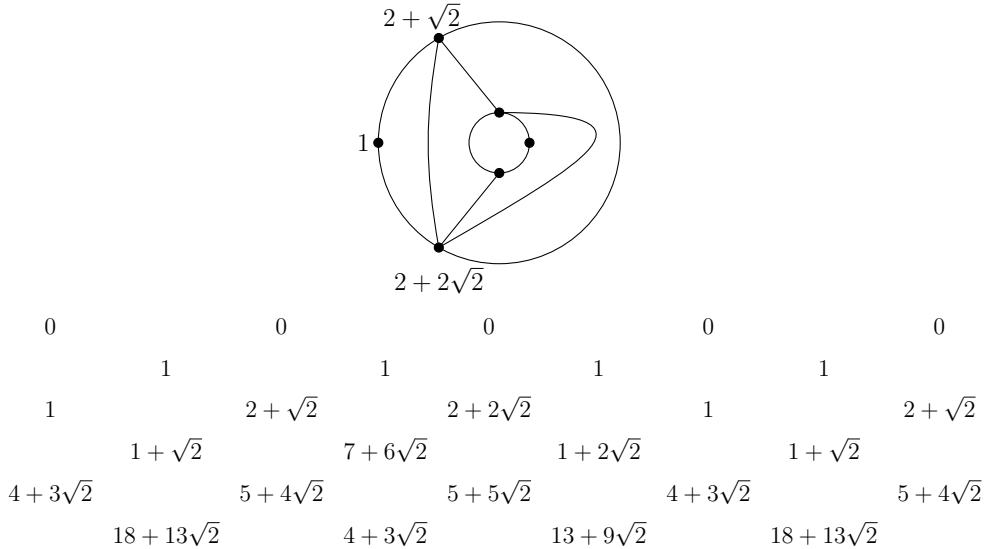
Definition 6. *Let S be a surface with nonempty boundary and let T be a cellular dissection of S . Fix one boundary component of S and label the vertices of this boundary component v_0, \dots, v_{n-1} in clockwise order. For each $0 \leq i \leq n-1$, let h_i be the intersection of a small circle centered at v_i with S . Let $\mu_p(i)$ denote the number of p -gons incident to v_i , where subgons intersected in multiple places by h_i contribute multiple times. Let F_T be the frieze pattern with quiddity row given by setting $F_T(i-1, i+1) = \sum_{p \geq 3} \mu_p(i) \lambda_p$.*

The following example highlights the use of h_i in the above definition.

Example 3. We apply [Definition 6](#) to a triangulation of P_6^\bullet . Notice that even though globally we see that the vertex labeled 7 is incident to 6 triangles, the “folded” triangle contributes 2 to the sum. The resulting frieze pattern is infinite; we display the first few rows.



We also illustrate the first few rows of an infinite frieze pattern from a dissection of an annulus.



Baur, Fellner, Parsons, and Tschabold studied the growth behavior of periodic, infinite frieze patterns. This growth is encoded in a family of integers, called *growth coefficients*, which measure how fast diagonals in the frieze pattern grow. Let $T_k(x)$ denote the k th normalized Chebyshev polynomial of the first kind, defined by the recurrence

$$T_k(x) = xT_{k-1}(x) - T_{k-2}(x) \text{ for } k \geq 2 \quad T_0(x) = 2 \quad T_1(x) = x.$$

Theorem 5 ([BFPT19]). *Let F be an infinite frieze pattern and let j be the minimal period of the quiddity row. Then, for all $k \geq 1$, $F(i, i + jk + 1) - F(i + 1, i + jk)$ is constant for all $i \in \mathbb{Z}$. Moreover, if s_k denotes this constant difference, then $s_k = T_k(s_1)$ for all $\ell \geq 1$.*

We will primarily focus on the first growth coefficient, s_1 , since determines all others. Sometimes s_1 is also called the *principal growth coefficient*. For example, using the minimal periods, we have that the principal growth coefficients in the first example is 2 and in the second example is $3 + 3\sqrt{2}$.

Baur, Parsons, and Tschabold gave a geometric model for all infinite, positive integral frieze patterns. The following is a combination of this characterization and a characterization of the growth coefficients.

Theorem 6 ([BPT16]). *All infinite, positive integral frieze patterns arise from a triangulation of P_n^\bullet or of an annulus. A frieze pattern arises from a triangulation of P_n^\bullet if and only if its principal growth coefficient is 2.*

Using the defining recurrence, we can see $T_k(2) = 2$ for all $k \geq 1$ and that either all growth coefficients of a frieze pattern are at least 2 or the frieze is not simultaneously positive, integral and infinite. Therefore, one can replace the last condition of the Theorem with the condition that *any* growth coefficient is 2.

The second author and Chen investigated infinite frieze patterns from dissections of P_n^\bullet and annuli. They gave a description of frieze patterns from general dissections via a “realizability algorithm” on the quiddity row. If the frieze pattern is of type Λ_{m+2} , the result simplifies to an $(m+2)$ -angulated version of Theorem 6.

Theorem 7 ([BC21]). *All infinite, positive frieze patterns of type Λ_{m+2} arise from an $(m+2)$ -angulation of P_n^\bullet or of an annulus. Moreover, an infinite frieze pattern arises from an $(m+2)$ -angulation of P_n^\bullet if and only if its principal growth coefficient is 2.*

We conclude this section with a combinatorial interpretation of entries of a frieze pattern from a dissection which will be useful in future proofs. Given a polygon P_n with dissection T , we say an (*admissible*) *matching* between v_i and v_j is a sequence Q_{i+1}, \dots, Q_{j-1} such that each Q_k is a subgon incident to v_k and such that each p -gon from the dissection appears on the list at most $p - 2$ times.

These matchings were introduced in the case of triangulations by Broline, Crowe, and Isaacs [BCI74]. They were extended to dissections by the second author and Chen in [BC21], inspired by a construction by Bessenrodt [Bes15]. For general dissections, there is a weight, denoted wt_T , associated to each matching based on the number of times every subgon appears on the list. We do not need the details here, beyond the fact that $wt_T(Q_{i+1}, \dots, Q_{j-1}) \geq 1$ and in the triangulation case, $wt_T(Q_{i+1}, \dots, Q_{j-1}) = 1$ for all admissible sequences, recovering the work of [BCI74].

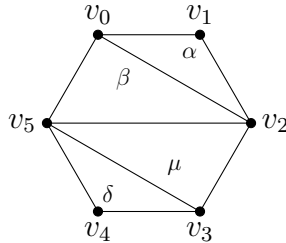
These constructions can be extended to frieze patterns from punctured polygons by lifting of P_n^\bullet with dissection T to a periodic dissection of an infinite strip. This was done in the triangulation case by Baur, Parsons, and Tschabold [BPT16] and in the dissection case in [BC21]. In this process, the vertex v_i lifts to a family of vertices $\{\overline{v}_{n\ell+i}\}_{\ell \in \mathbb{Z}}$. An arc of the form (v_i, v_j) lifts to the family of arcs between lifts of v_i and v_j . Meanwhile, spokes lift to an infinite family of *asymptotic arcs*, which have one endpoint and travel infinitely far in one direction in the disc. An example is given in [Example 4](#).

We summarize all of these results in the following, focusing only on the cases we will use.

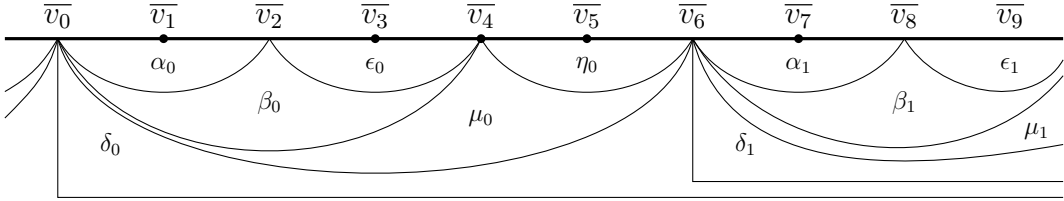
Theorem 8 ([BC21, BPT16, BCI74]).

- (1) *If F_T is the finite frieze pattern from a dissection T of a polygon P_n , then $F_T(i, j)$ is the weighted sum, under wt_T , of admissible matchings between v_i and v_j .*
- (2) *If F_T is the infinite frieze pattern from a dissection T of a once-punctured polygon P_n^\bullet , then $F_T(i, j)$ is the weighted sum, under wt_T , of admissible matchings between \overline{v}_i and \overline{v}_j in the lift of (P_n^\bullet, T) to the infinite strip.*

[Example 4](#). Here, we illustrate both parts of [Theorem 8](#). Below, we reproduce the triangulation from [Example 2](#), with vertices and subgons labeled. Using this indexing, we have $F(1, 4) = 5$, and 5 is also the cardinality of the admissible matchings between v_1 and v_4 . These are $\alpha, \mu; \alpha, \delta; \beta, \mu; \beta, \delta$; and μ, δ .



Next, we consider the triangulation T of P_6^\bullet in [Example 3](#). Below, we draw its lift to the universal strip and we again label the subgons. The subgons labeled δ_i have one endpoint at $+\infty$. With this indexing, $F_T(3, 9) = 5$, which is the cardinality of admissible matchings between \overline{v}_4 and \overline{v}_8 . These are $\eta_0, \mu_0, \alpha_1; \eta_0, \delta_0, \alpha_1; \eta_0, \delta_1, \alpha_1; \eta_0, \mu_1, \alpha_1$; and $\eta_0, \beta_1, \alpha_1$. For another example, we have $F_T(0, 4) = 1$, and there is a unique admissible matching between \overline{v}_0 and \overline{v}_4 , namely, $\alpha_0, \beta_0, \epsilon_0$.



4.2. Counting Frieze Patterns up to Symmetry. Our goal in this section is to enumerate frieze patterns in several ways. In particular, we will enumerate finite frieze patterns up to global row shift, and we will enumerate certain infinite frieze patterns. This will use an alternate description of the cyclic sieving phenomenon. The equivalence of the following and [Definition 1](#) is shown in [\[RSW04\]](#).

Proposition 6 ([\[RSW04\]](#)). *A triple $(X, G_n = \langle \sigma \rangle, f(q))$ exhibits the cyclic-sieving phenomenon if and only if each of the coefficients g_i determined by*

$$X(q) \equiv \sum_{i=0}^{n-1} g_i q^i \pmod{q^n - 1}$$

are equal to the number of G -orbits on X for which the stabilizer-order divides i .

Now, once we show that the operations of rotating a dissection T and shifting all rows in F_T agree, we can use [Proposition 6](#) to enumerate equivalence classes of frieze patterns. In the case of frieze patterns of type Λ_{m+2} , this largely follows from combining existing literature.

Lemma 6. *If T and T' are two dissections of P_n or P_n^\bullet where T' is the result of rotating T by $2\pi/n$ in the counterclockwise direction, then for all $0 \leq j - i \leq n$, $F_{T'}(i, j) = F_T(i+1, j+1)$.*

Proof. The statement is trivial for the first two rows, and by construction of F_T and $F_{T'}$ it is clear for the quiddity row. Now, if $j - i > 2$, this can be shown with [Lemma 5](#). \square

Conway and Coxeter showed that the rows in a frieze pattern of width n must be n -periodic. Hence, global row shift is a cyclic action on the set of frieze patterns of fixed width, and one can easily export any cyclic sieving phenomenon from dissections of P_n to frieze patterns of width n .

We will now turn our attention to utilizing the cyclic sieving phenomenon to enumerate equivalence classes of frieze patterns. In the following, if $n = m\ell + 2$, let $\tilde{c}_\ell^{(m)}(q)$ denote the degree $n - 1$ polynomial which is equivalent to $c_\ell^{(m)}(q)$ modulo $q^n - 1$.

Proposition 7. *Let m be a positive integer and let $n = m\ell + 2$. The number of equivalence classes of positive frieze patterns of type Λ_{m+2} and of width n up to global row shift is the constant term of $\tilde{c}_\ell^{(m)}(q)$.*

Proof. First, let $m = 1$. By [\[RSW04, Theorem 7.1\]](#), the triple $(\mathcal{T}_n, G_n, c_{n-2}(q))$ exhibits the cyclic sieving phenomenon where \mathcal{T}_n is the set of triangulations of P_n . By [Proposition 6](#), this means that the constant term of $\tilde{c}_{n-2}^{(1)}(q) \pmod{q^n - 1}$ is equal to the total number of cyclic equivalence classes of triangulations of P_n . Then, [Theorem 3](#) and [Lemma 6](#) imply that these equivalence classes are in bijection with equivalence classes of positive, integral frieze patterns of width n up to global row shift.

If $m > 1$, the same logic holds, applying instead the cyclic sieving result in [EF08, Theorem 3.8] and the bijection in [Theorem 4](#). \square

Remark 2. A triangulation T of P_n determines a cluster in a type A_{n-3} cluster algebra, \mathcal{A} , as well as a cluster-tilting object S_T in the associated cluster category, $\mathcal{C}_{\mathcal{A}}$ [CCS06]. One can go from the $\mathcal{C}_{\mathcal{A}}$ to \mathcal{A} using a *cluster character map*, as was first defined in [CC06]. Palu described how to build a cluster character map for any given cluster-tilting object [Pal08].

It is common to draw the *Auslander-Reiten (AR) quiver* of $\mathcal{C}_{\mathcal{A}}$ which has vertices labeled by indecomposable objects and which has the same overall shape as the frieze pattern F_T . Indeed, one can view F_T as the result of applying the cluster character map associated to S_T to each vertex/object in the AR quiver, yielding cluster variables (in particular, Laurent polynomials), then further specializing the initial variables in each expression to 1, yielding integers.

Rotation of P_n also has a meaning in this setting; it coincides with *Auslander-Reiten (AR) translation*, an important and prominent functor on $\mathcal{C}_{\mathcal{A}}$. Therefore, studying equivalence classes of positive integral, finite frieze patterns under rotation/global row shift is equivalent to studying equivalence classes of cluster character maps associated to cluster tilting objects under AR translation.

This remark does not hold for the positive integral, infinite frieze patterns considered here as our action does not coincide with AR translation anymore. See [Proposition 3](#).

Next, fix a positive integer n and a finite set $\mathcal{M} = \{m_1, \dots, m_s\} \subset \mathbb{Z}_{>0}$. Let $a_{\mathcal{M}}(q) := \sum_{\mu} a_{\mu}(q)$ where we sum over all $\mu = (\mu_1, \dots, \mu_n) \in \mathbb{Z}^n$ such that $\sum i\mu_i = n - 2$ and $\mu_i > 0$ only if $i \in \mathcal{M}$. By construction, $a_{\mathcal{M}}(1)$ is the number of dissections of an n -gon which only use subgons with sizes from \mathcal{M} . Let $\tilde{a}_{\mathcal{M}}(q)$ denote the degree $n - 1$ polynomial which is equivalent to $a_{\mathcal{M}}(q)$ modulo $q^n - 1$.

Proposition 8. *Fix a positive integer n and a finite set $\mathcal{M} = \{m_1, \dots, m_s\} \subset \mathbb{Z}_{>0}$. The number of equivalence classes of frieze patterns from dissections of width n and with values in $\mathbb{Z}[\lambda_{m_1+2}, \dots, \lambda_{m_s+2}]$ up to global shift of rows is the constant term of $\tilde{a}_{\mathcal{M}}(q)$.*

Proof. This result follows from [Theorem 1](#), [Proposition 6](#), and [Lemma 6](#). \square

Next, we use our cyclic sieving result on dissections of P_n^{\bullet} to count infinite frieze patterns of type Λ_{m+2} with a fixed minimal period of their rows. Neither [Theorem 6](#) nor [Theorem 7](#) is phrased as a bijection. This is because, given a dissection T of P_n^{\bullet} or an annulus, we can construct a k -fold dilation of T for any $k \geq 1$ which would yield the same frieze pattern. The two dissections in [Figure 2](#) are examples of this process. This dilation will not change the type of underlying surface, and a consequence of the constructive proofs in [BC21, BPT16] is that there is a dissection associated to a minimal period of the quiddity row.

Recall we have assumed that all infinite frieze patterns are periodic. A consequence of [Lemma 5](#) is that the period of any row will divide the period of the quiddity row. Therefore, the period of the quiddity row is the *minimal period* of all rows of an infinite frieze pattern.

We begin by considering the integral case, for which we have a complete result. Let $\tilde{t}_n(q)$ denote the unique polynomial of degree $n - 1$ which is equivalent to $t_n(q)$ modulo $q^n - 1$.

Theorem 9. *The number of infinite, positive integral frieze patterns with principal growth coefficient 2 and minimal period n , counted up to global shift of the rows, is $[q^1]\tilde{t}_n(q)$. Equivalently, the number of infinite, positive integral frieze patterns with rows with principal growth coefficient 2 and minimal period n is $n[q^1]\tilde{t}_n(q)$.*

Proof. An infinite, positive integral frieze pattern with principal growth coefficient 2 with whose rows are n -periodic arises from a triangulation T of P_n^\bullet by [Theorem 6](#). If n is the minimal period of the rows, then T is not a k -fold dilation of a triangulation T' of $P_{n'}^\bullet$ with $n' < n$. This is equivalent to saying that T does not have nontrivial rotational symmetry. Therefore, the stabilizer of T in $G_n = \langle \sigma \rangle$, the cyclic group acting on triangulations of P_n^\bullet by rotation, is the identity element. Combining [Proposition 3](#) and [Proposition 6](#) shows that the number of such orbits is the linear term of $t_n(q)$.

If we want to count all such frieze patterns instead of grouping them by shift equivalence classes, we can simply multiply this number by n . The absence of symmetry in these dissections ensures this does not overcount. \square

The sequence $[q^1]\tilde{t}_n(q)$ begins 1, 1, 3, 8, 27, 245, 800, ... and appears to coincide with [OEIS A022553](#). The sequence $n[q^1]\tilde{t}_n(q)$ also seems to appear as [OEIS A045630](#).

Question 3. *Can infinite, positive integral frieze patterns with principal growth coefficient $s > 2$ for a fixed s be counted in a similar way?*

When considering $(m+2)$ -angulations for $m > 1$, due to the restriction in [Proposition 2](#), we cannot consider all possible numbers of spokes. In order to convert our result on $(m+2)$ -angulations of P_n^\bullet to a result about frieze patterns, we explain how the number of spokes of a dissection affects the associated frieze pattern. In the following, note that a *fundamental domain* of an infinite frieze pattern F_T with n -periodic rows is an infinite set of the form $\{F_T(i, j) : k \leq i \leq k+n-1, j \geq i\}$ for any $k \in \mathbb{Z}$.

Proposition 9. *If F_T is an infinite frieze pattern of type Λ_{m+2} associated to a dissection $T \in T_{n,s}^{\bullet,(m)}$, then there are $\frac{n}{m} - s$ entries 1 in any fundamental domain of F_T .*

Proof. In [\[BCI74, Corollary 2\]](#), Broline, Crowe, and Isaacs show that, given a polygon P_n with triangulation T , if $(v_i, v_j) \in T$, then there is only one admissible matching between v_i and v_j . The same argument holds in the more general case of a polygon with dissection.

Recall that when working with a frieze pattern from a dissection T of P_n^\bullet , we first construct a lift of T to the infinite strip. However, every arc in the infinite strip can be regarded as a diagonal in a finite polygon inside the strip, allowing us to use the same machinery as in the finite case. Since spokes lift to one-sided infinite arcs with only one endpoint, entries of 1 in an infinite frieze pattern from a dissection of P_n^\bullet will correspond to lifts of non-spokes. Each non-spoke from T will correspond to one entry in a fundamental domain of F_T . An $(m+2)$ -angulation of P_n^\bullet will use $\frac{n}{m}$ arcs, so there will be $\frac{n}{m} - s$ non-spokes. By our previous discussion, we can conclude there are $\frac{n}{m} - s$ entries 1 in a fundamental domain of F_T . \square

Let $\tilde{t}_{n,s}^{(m)}(q)$ denote the unique polynomial of degree $n-1$ which is equivalent to $t_{n,s}^{(m)}(q)$ modulo $q^n - 1$.

Proposition 10. *Let n, m , and s be a triple satisfying the conditions from [Proposition 4](#). The number of infinite frieze patterns of type Λ_{m+2} with growth coefficient 2 having minimal period n and $\frac{n}{m} - s$ entries 1 in any fundamental domain, counted up to global shift of the rows, is $[q^1]\tilde{t}_{n,s}^{(m)}(q)$. Equivalently, the total number of infinite frieze patterns of type Λ_{m+2} with growth coefficient 2 having minimal period n and $\frac{n}{m} - s$ entries 1 in any fundamental domain is $n[q^1]\tilde{t}_{n,s}^{(m)}(q)$.*

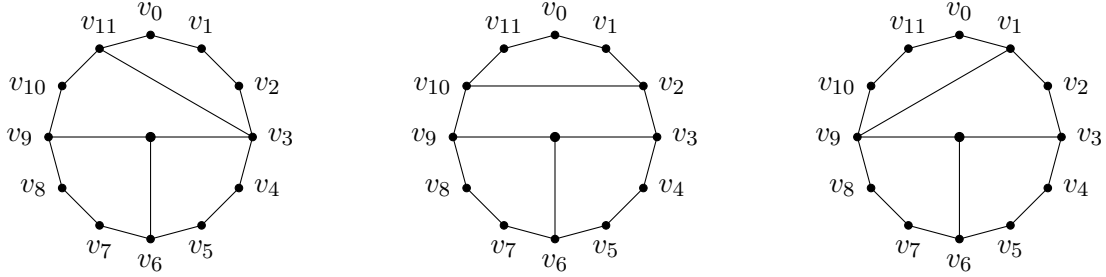


FIGURE 3. Representatives for the three symmetry classes of infinite frieze patterns of type Λ_5 with one 1 in any fundamental domain and minimal period 12.

The proof of [Proposition 10](#) is analogous to that of [Theorem 9](#).

Example 5. As previously noted, the triple $n = 12, m = 3, s = 3$ satisfies the conditions in [Proposition 4](#). Therefore, the number of infinite frieze patterns of type Λ_5 with growth coefficient 2, minimal period 12, and one entry 1 in any fundamental domain, counted up to global shift, is $[q^1]t_{12,3}^{(4)} = [q^1](3 \left[\begin{smallmatrix} 12 \\ 11 \end{smallmatrix} \right]_q) = 3$. Equivalently, the total number of such frieze patterns (no longer counting up to shift) is 36. We draw 5-angulation representatives of the three symmetry classes in [Figure 3](#).

4.3. Frieze patterns from orbifolds. In this section, we discuss an interpretation of frieze patterns from triangulations with nontrivial symmetry. A triangulated polygon either has no rotational symmetry, 2-fold rotational symmetry, or 3-fold rotational symmetry. The corresponding frieze patterns correspond with three of the four types of friezes with glide symmetry; see [\[CC73a, CC73b, Questions \(3\)-\(5\)\]](#).

These three cases can also be explained by extending the notion of growth coefficients to finite frieze patterns. By insisting that a frieze pattern is tame (recall [Definition 4](#)) and allowing negative entries, every finite frieze pattern can be uniquely extended to an infinite frieze pattern. In particular, in such an extension, the row beneath the bottom row of 0's would consist of -1 's.

The following was suggested in [\[BFPT19, Proposition 5.9\]](#). We fill in some details to prove this in general. We will heavily use item (1) from [Theorem 8](#).

Proposition 11. *Let F be a finite, positive integral frieze pattern of width n and let T be the corresponding triangulation of P_n ; that is, $F = F_T$.*

- (1) *The principal growth coefficient of F is -2 if and only if T has no nontrivial rotational symmetry.*
- (2) *The principal growth coefficient of F is 0 if and only if T has 2-fold rotational symmetry.*
- (3) *The principal growth coefficient of F is 1 if and only if T has 3-fold rotational symmetry.*

Proof. Since every triangulation with rotational symmetry has 2-fold or 3-fold symmetry and every frieze pattern corresponds uniquely to a triangulation, it will suffice to show the three “if” statements hold.

Item (1) Saying T has no nontrivial rotational symmetry is equivalent to saying that the quiddity row of F_T has minimal period n . In the extension of F_T to an infinite frieze pattern,

$F(i, i+n+1) = -1$ for all i , and we see the growth coefficient is $F(i, i+n+1) - F(i, i+n-1) = -1 - 1 = -2$.

Item (2) Saying T has 2-fold rotational symmetry is equivalent to saying that the quiddity row of F_T has minimal period $\frac{n}{2}$. By [Theorem 8](#), $F(0, \frac{n}{2} + 1)$ is equal to the number of admissible matchings between v_0 and $v_{\frac{n}{2}+1}$ and $F(1, \frac{n}{2})$ is equal to the number of admissible matchings between v_1 and $v_{\frac{n}{2}}$. By [\[BCI74, Corollary 1\]](#), the number of admissible matchings between v_0 and $v_{\frac{n}{2}+1}$ (i.e choosing subgons at $v_1, v_2, \dots, v_{\frac{n}{2}}$) is equivalent to the number of admissible matchings between $v_{\frac{n}{2}+1}$ and v_0 (i.e choosing subgons at $v_{\frac{n}{2}+2}, v_{\frac{n}{2}+3}, \dots, v_{n-1}$). The latter is equal to the number of admissible matchings between v_1 and $v_{\frac{n}{2}}$ because T has 2-fold symmetry. Therefore, $F(0, \frac{n}{2} + 1) - F(1, \frac{n}{2}) = 0$, and by [Theorem 5](#), 0 is the principal growth coefficient.

Item (3) If T has 3-fold rotational symmetry, then the quiddity row of F_T has minimal period $\frac{n}{3}$. Such a triangulation will have a central triangle, so without loss of generality, suppose this triangle consists of diagonals $(v_0, v_{\frac{n}{3}})$, $(v_{\frac{n}{3}}, v_{\frac{2n}{3}})$, and $(v_{\frac{2n}{3}}, v_0)$. We again compare admissible matchings between v_0 and $v_{\frac{n}{3}+1}$ with admissible matchings between v_1 and $v_{\frac{n}{3}}$. We can regard the latter pair of vertices inside the smaller polygon formed by $v_0, v_1, \dots, v_{\frac{n}{3}}$, with the diagonal $(v_0, v_{\frac{n}{3}})$ a boundary edge; call this polygon Q . Applying [\[BCI74, Corollary 1\]](#) to the computation of $F(1, \frac{n}{3})$ inside Q , we have that the number of admissible matchings between v_1 and $v_{\frac{n}{3}}$ can be computed by counting the number of subgons in Q incident to v_0 . That is, we have shown $F(1, \frac{n}{3}) = 1 + \#\{(v_0, v_i) \in T : 0 < i < \frac{n}{3}\}$.

Now, we consider admissible matchings between v_0 and $v_{\frac{n}{3}+1}$. By [\[BCI74, Corollary 2\]](#), there is a unique admissible matching between v_0 and $v_{\frac{n}{3}}$, and this uses every subgon in Q . Therefore, an admissible matching between v_0 and $v_{\frac{n}{3}+1}$ is the result of appending a subgon incident to $v_{\frac{n}{3}}$ which is not in Q to this sequence. The number of such subgons is $1 + \#\{(v_{\frac{n}{3}}, v_i) \in T : \frac{n}{3} < i < n\} = 2 + \#\{(v_{\frac{n}{3}}, v_i) \in T : \frac{n}{3} < i < \frac{2n}{3}\}$, where we use our assumption about the position of the central triangle. Since T has 3-fold symmetry, we know $\#\{(v_{\frac{n}{3}}, v_i) \in T : \frac{n}{3} < i < \frac{2n}{3}\} = \#\{(v_0, v_i) \in T : 0 < i < \frac{n}{3}\}$, so $F(0, \frac{n}{3} + 1) - F(1, \frac{n}{3}) = 1$. \square

Remark 3. [Proposition 11](#) could easily be extended by associating to a dissection T the largest ℓ such that T has ℓ -fold symmetry. For $\ell > 3$, we can use the same strategy as in the proof of Item (3), utilizing the combinatorial interpretation of entries of F_T from [\[BC21\]](#). We chose to focus on the case of integral frieze patterns and triangulations since the motivation of this section comes from the theory of generalized cluster algebras, whose generators will always specialize to integers by the Laurent Phenomenon [\[CS14\]](#).

[Proposition 11](#) partitions finite, positive integral frieze patterns into three sets. Our goal in the remainder of this section is to discuss an interpretation of frieze patterns described in items (2) and (3). This will require a new perspective on frieze patterns.

In [\[HJ20, Theorem 1.5\]](#), Holm and Jørgensen show that the values F_T in a frieze pattern associated to a dissection T of a polygon satisfy Ptolemy relations. That is, for all $i < j < k < \ell$, we have

$$F_T(i, k)F_T(j, \ell) = F_T(i, j)F_T(k, \ell) + F_T(i, \ell)F_T(j, k).$$

Given T a dissection of P_n , each frieze pattern F_T encodes a ring homomorphism from a *type A_{n-3} cluster algebra* to $\mathbb{Z}[\lambda_{p_1}, \dots, \lambda_{p_s}]$ where p_1, \dots, p_s are the sizes of the subgons cut out by T . This follows from the geometric realization of these algebras [\[FZ03, Section 12.2\]](#).

Studying homomorphisms from more general cluster algebras to integral domains has been a topic of interest lately; see for example [\[QFGET22, FT24, FP16, GHL23, GS20\]](#). These

homomorphisms are called *friezes*. Often, the cluster algebras studied through the lens of friezes have a geometric realization, allowing a pictorial description of the homomorphism. In particular, friezes on P_n with positive integral values are in bijection with frieze patterns of width n with positive integral values.

We will introduce a new family of friezes here which will correspond to the frieze patterns in [Proposition 11](#) items (2) and (3). These are related to skew-symmetrizable cluster algebras and generalized cluster algebras in the sense of Chekhov-Shapiro [[CS14](#)] respectively. We will define these purely geometrically and avoid relying on the language of cluster algebras.

An orbifold is a generalization of a manifold with singular points called orbifold points. Let P_n^* denote a polygon P_n with one orbifold point \star which has an order $p \geq 2$. Arcs on P_n^* are equivalence classes of sets of arcs on P_{pn} which are fixed under $2\pi/p$ rotation. Triangulations on P_n^* come from maximal sets of arcs on P_{pn} which are invariant under rotation.

The family of arcs generated by all rotations of $(i, i + n)$, $0 \leq i < n$, project to an arc γ on P_n^* with $\gamma(0) = \gamma(1) = v_i$ such that γ cuts out a monogon containing \star . We refer to these as *pending arcs*. Note that some other sources will instead draw pending arcs as having an endpoint at v_i and an endpoint at \star ; we forbid such curves and insist our arcs only have endpoints in marked points, i.e. vertices. We use the same conventions as in the description of arcs on P_n^* . Here, the notation (v_i, v_i) will mean the pending arc based at v_i ; non-pending arcs will be called *standard arcs* for emphasis.

Consider a function f on the set of arcs of P_n^* . Given two arcs τ, τ' which intersect, we say that the product $f(\tau)f(\tau')$ respects *skein relations* if $f(\tau)f(\tau') = f(\Gamma^+) + f(\Gamma^-)$ where Γ^+ and Γ^- are sets of arcs resulting from taking the chosen intersection point X of τ and τ' and replacing it with \asymp and \circ respectively. When performing this smoothing on an orbifold it is possible to produce a curve with a self-intersection. In this case, one proceeds by smoothing the self-crossing in the same way. Smoothing a self-crossing will produce a closed curve ξ which is either contractible closed curve or which encloses \star . In the former case, we set $f(\xi) = -2$ and in the latter we set $f(\xi) = \lambda_p$ where p is the order of \star . In particular, in the case of P_n^* , performing this process for two distinct pending arcs, which will have two points of intersection, yields

$$(3) \quad f(v_i, v_i)f(v_j, v_j) = f(v_i, v_j)^2 + \lambda_p f(v_i, v_j)f(v_j, v_i) + f(v_j, v_i)^2.$$

Definition 7. Given an integral domain R , a *frieze* on a surface or orbifold (S, M) is a function $f : \{\text{arcs on } (S, M)\} \rightarrow R$ such that

- $f(\gamma) = 1$ if γ is isotopic to a boundary segment and
- f respects skein relations.

If all values of f lie in $\mathbb{Z}_{>0}$, we say f is a *positive integral frieze*.

An important question in the study of friezes is whether every frieze over a fixed surface or orbifold is *unitary*. A frieze on (S, M) is unitary if there exists a triangulation T such that $f(\tau) = 1$ for all $\tau \in T$. Since this uniquely determines the frieze, we denote this f_T . Fontaine and Plamondon show that friezes on P_n^* are not always unitary [[FP16](#)]. Felikson and Tumarkin recently showed that every frieze on an unpunctured surface is unitary and classified friezes for general surfaces [[FT24](#)].

If \star is order 2, then standard arcs on P_n^* correspond to centrally symmetric pairs of arcs on P_{2n} while pending arcs correspond to diameters (v_i, v_{n+i}) . Centrally symmetric triangulations of P_{2n} provide a geometric realization for cluster algebras of type C_{n-1} . Using the technique of folding Dynkin diagrams, Fontaine and Plamondon showed the following.

Proposition 12 ([FP16]). *Given a positive integral orbifold frieze f on P_n^* where \star is an orbifold point of order 2, there exists a unique triangulation T of P_n^* such that for all $\tau \in T$, $f(\tau) = 1$.*

Proof. A frieze on P_n^* when \star has order 2 is equivalent to a frieze of type C_{n-1} . Fontaine and Plamondon show that such friezes are in 1-1 correspondence with friezes on P_{2n} associated to centrally symmetric triangulations [FP16]. Equivalently, each frieze on P_n^* is of the form f_T for T a triangulation of P_n^* . \square

The case of order 2 is special because $\lambda_2 = 0$, so one term in [Equation \(3\)](#) disappears. The natural next candidate to consider is order 3. Our proof in this case is inspired by the proof for friezes on P_n , which is given in [CC73a, CC73b, Question 25].

Proposition 13. *Given a positive integral orbifold frieze f on P_n^* where \star is an orbifold point of order 3, there exists a unique triangulation T of P_n^* such that for all $\tau \in T$, $f(\tau) = 1$.*

Proof. We will induct on n . The case of P_1^* is trivial because there are no non-boundary arcs on P_1^* . We also directly check P_2^* . Here, there are two non-boundary arcs, (v_0, v_0) and (v_1, v_1) whose values under any frieze f satisfy $f(v_0, v_0)f(v_1, v_1) = f(v_0, v_1)^2 + f(v_0, v_1)f(v_1, v_0) + f(v_1, v_0)^2 = 3$. We see that we must have either $f(v_0, v_0) = 1$ and $f(v_1, v_1) = 3$ or the same with the roles of v_0 and v_1 swapped. In each case, the single arc with value 1 under the frieze forms a triangulation of P_2^* .

Now, we assume we have shown our claim for P_{n-1}^* and we consider a frieze on P_n^* . Assume for sake of contradiction that for all $0 \leq i \leq n-1$, $f(v_{i-1}, v_{i+1}) > 1$. For all $2 \leq i \leq n-1$, we have $f(v_0, v_i)f(v_{i-1}, v_{i+1}) = f(v_0, v_{i-1}) + f(v_0, v_{i+1})$. In other words,

$$f(v_0, v_{i+1}) = f(v_0, v_i)f(v_{i-1}, v_{i+1}) - f(v_0, v_{i-1}) \geq 2f(v_0, v_i) - f(v_0, v_{i-1}).$$

Similarly, the skein relation $f(v_0, v_{n-1})f(v_{n-2}, v_0) = f(v_0, v_0) + f(v_0, v_{n-2})$ yields

$$f(v_0, v_0) = f(v_0, v_{n-1})f(v_{n-2}, v_0) - f(v_0, v_{n-2}) \geq 2f(v_0, v_{n-1}) - f(v_0, v_{n-2}).$$

Therefore, we have a chain of inequalities,

$$f(v_0, v_0) - f(v_0, v_{n-1}) \geq f(v_0, v_{n-1}) - f(v_0, v_{n-2}) \geq \dots \geq f(v_0, v_2) - f(v_0, v_1) \geq 2 - 1 > 0$$

implying

$$f(v_0, v_0) > f(v_0, v_{n-1}) > \dots > f(v_0, v_2) > 1.$$

We can replace v_0 with any other vertex and get a similar chain of inequalities. Now, suppose we have indexed the vertices so that $f(v_0, v_0) = \min\{f(v_j, v_j) : 0 \leq j \leq n-1\}$. Apply the skein relation from [Equation \(3\)](#) to the intersections between (v_0, v_0) and (v_{n-1}, v_{n-1}) ,

$$\begin{aligned} f(v_0, v_0)f(v_{n-1}, v_{n-1}) &= f(v_0, v_{n-1})^2 + f(v_0, v_{n-1})f(v_{n-1}, v_0) + f(v_{n-1}, v_0)^2 \\ &= f(v_0, v_{n-1})^2 + f(v_0, v_{n-1}) + 1 \end{aligned}$$

By our designation of v_0 , we have

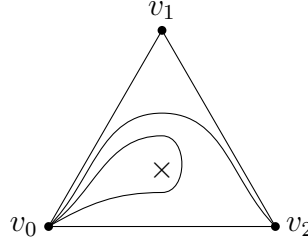
$$(4) \quad f(v_0, v_{n-1})^2 + f(v_0, v_{n-1}) + 1 \geq f(v_0, v_0)^2.$$

Recall we have shown $f(v_0, v_0) > f(v_0, v_{n-1})$. Since $n \geq 3$, we have that $f(v_0, v_0) \geq 3$ and $f(v_0, v_{n-1}) \geq 2$, and we can conclude that [Equation \(4\)](#) is impossible.

From this contradiction, we see there must exist a value $0 \leq i \leq n-1$ such that $f(v_{i-1}, v_{i+1})$ is 1. Restricting to values $f(v_j, v_k)$ for $0 \leq j, k \leq n-1, j \neq i \neq k$ gives a frieze on P_n^* where the edge (v_{i-1}, v_{i+1}) behaves as a boundary arc. By the inductive hypothesis, there

exists a triangulation T' of this copy of P_{n-1}^* such that for all $\tau \in T'$, $f(\tau) = 1$. Therefore, $T := T' \cup \{(v_{i-1}, v_{i+1})\}$ is also such a triangulation f , showing f is unitary. \square

Example 6. Let T be the triangulation of P_3^* given below.



We display the entries of the frieze associated to this triangulation in the table below for \star both order 2 and order 3, where the entry in row v_i and column v_j is $f(v_i, v_j)$.

\star has order 2				\star has order 3			
$v_i \setminus v_j$	v_0	v_1	v_2	$v_i \setminus v_j$	v_0	v_1	v_2
v_0	1	1	1	v_0	1	1	1
v_1	2	5	1	v_1	2	7	1
v_2	1	3	2	v_2	1	4	3

One can check that [Equation \(3\)](#) holds for these values as well as other skein relations. For instance, when \star is order 3, we see

$$f(v_1, v_1)f(v_2, v_2) = 7 \times 3 = 4^2 + 1 \times 4 \times 1 + 1^2 = f(v_2, v_1)^2 + \lambda_3 f(v_2, v_1)f(v_1, v_2) + f(v_1, v_2)^2.$$

Knowing that friezes on P_n^* are unitary when \star is order 2 or 3 allows us to identify each with a finite positive integral frieze pattern.

Corollary 3.

- (1) *There is a 1-1 correspondence between positive integral frieze patterns with width $2n$ and principal growth coefficient 0 and friezes on P_n^* where \star has order 2.*
- (2) *There is a 1-1 correspondence between positive integral frieze patterns with width $3n$ and principal growth coefficient 1 and friezes on P_n^* where \star has order 3.*

Proof. By [Proposition 11](#), finite frieze patterns with principal growth coefficient 0 are in 1-1 correspondence with centrally symmetric triangulations, and these are in correspondence with triangulations of P_n^* where \star is order 2. By [Proposition 12](#), these triangulations are in 1-1 correspondence with friezes on P_n^* . This shows statement (1), and statement (2) is analogous, where we instead use [Proposition 13](#). \square

5. FRIEZE PATTERNS AND DYCK PATHS

We have so far explored correspondences between dissections of polygons and frieze patterns with a particular eye towards the compatibility of the symmetries of each object. In this section, we will export this narrative to the setting of Dyck paths. In particular, we will highlight the action on m -Dyck paths induced by rotation of $(m+2)$ -angulations of polygons.

A Dyck path is a certain type of lattice path. These are a well-known family of Catalan objects and hence are equinumerous with triangulations of polygons and finite, positive integral frieze patterns. In order to discuss $(m+2)$ -angulations for $m > 1$, we will recall the more general notion of m -Dyck paths.

Definition 8. An m -Dyck path of order ℓ is a sequence of steps in direction $(0, 1)$ (denoted U) or $(1, 0)$ (denoted R) from $(0, 0)$ to $(m\ell, \ell)$ which stays above the $y = \frac{1}{m}x$ diagonal line.

See the left-hand side of Figure 5 for an example of a 2-Dyck path. We remark that it is natural to conflate the lattice paths of an m -Dyck path with the m -Dyck path itself, and we will do this at times.

When $m = 1$, Definition 8 recovers that of standard Dyck paths. In general, the number of m -Dyck paths of order ℓ is equal to the Fuss-Catalan number $c_\ell^{(m)}$.

Let $D = w_1, \dots, w_d$ be an m -Dyck path; i.e., each $w_i \in \{U, R\}$. It is useful to note that the property of staying above the line $y = \frac{1}{m}x$ is equivalent to the property that the number of R 's in any initial subsequence w_1, \dots, w_k is no greater than m times the number of U 's. Such a sequence can be referred to as *m-ballot* or *m-Yamaouchi*.

Our first goal is to recall a bijection between m -Dyck paths of order ℓ and $(m+2)$ -angulations of $P_{m\ell+2}$, described in [Eth40]; see also the description in [Sta96].

Recall the vertices of P_n are labeled v_0, \dots, v_{n-1} in clockwise order. Let $\mathcal{T}_{m\ell+2}^{(m)}$ denote the set of $(m+2)$ -angulations of $P_{m\ell+2}$ and let $\mathcal{D}_\ell^{(m)}$ denote the set of m -Dyck paths of order ℓ .

Definition 9. We define the browse map $\text{brow} : \mathcal{T}_{m\ell+2}^{(m)} \rightarrow \mathcal{D}_\ell^{(m)}$ by associating to each $T \in \mathcal{T}_{m\ell+2}^{(m)}$ the word $\text{brow}(T)$ determined by performing the following steps in the prescribed order. Walk clockwise around $P_{m\ell+2}$, beginning at v_0 and visiting each vertex. During the visit of v_i , survey the incident subgons, sweeping in counterclockwise order. There are three possible cases when we encounter a subgon Q , and we outline the effect to the word in Figure 4.

Case for an $(m+2)$ -gon Q incident to a vertex of P_n	Modification to the word
Case 1: This is the first time we see Q .	Append a U .
Case 2: This is neither the first time nor the $(m+2)$ -th time we see Q .	Append an R .
Case 3: This is the $(m+2)$ -th time we see Q .	Append nothing.

FIGURE 4. An outline of the choices for building an m -Dyck path from an $(m+2)$ -angulation of a polygon.

Using the algorithm in Definition 9 yields the 2-Dyck path on the right of Figure 5 from the 4-angulation on the left. For instance, v_0 is incident to two subgons and naturally this is the first time we seen each subgon, hence the Dyck path begins with two up steps. Then, v_1 is incident to one of these subgons which was already viewed by v_0 and a new subgon, so the path continues with a right step and another up step.

The fact that the word $\text{brow}(T)$ indeed determines an m -Dyck path was proven in [Eth40]. We will next define a map which will be shown to be the inverse to the browse map. First, we introduce some terminology and conventions for m -Dyck paths. Call a lattice point on a Dyck path a *corner* if it is incident to both an up step and a right step and let all other lattice points be *non-corners*.

Definition 10. Given an m -Dyck path of order ℓ , create a multiset of size $\ell - 1$ of lines of slope $\frac{1}{m}$, with one passing through the lowest point of each up step, excluding the first up step. The lines in the multiset are called balance lines.²

There are four balance lines drawn with dotted lines on the left in [Figure 5](#), where the middle one comes with multiplicity 2 as it goes through two corners. The teal balance line and its first intersection with a non-corner will be of extra importance in [Theorem 10](#), hence the star at its end.

Let l be a balance line of an m -Dyck path. If l begins at point (i, i') and first intersects a non-corner of D at (j, j') then we *label* l with the pair $(i, j+1)$. For instance, the teal balance line in [Figure 5](#) is labeled $(0, 9)$, the two red balance lines are labeled $(1, 8)$ and $(3, 8)$, and the orange balance line is labeled $(3, 6)$. One subtle point worth emphasizing is that each up step which is incident to the diagonal $y = \frac{1}{m}x$ has its first intersection with a non-corner at the terminal point $(m\ell, \ell)$. Therefore, each such balance line is labeled $(i, m\ell + 1)$ where i is necessarily positive by our convention in [Definition 10](#).

Definition 11. We define the return map $\text{rtn} : \mathcal{D}_\ell^{(m)} \rightarrow \mathcal{T}_{m\ell+2}^{(m)}$ by associating to each m -Dyck path D the $(m+2)$ -angulation $\text{rtn}(w)$ given by diagonals $\{(v_i, v_j)\}$ where $\{(i, j)\}$ is the set of labels of balance lines of D .

The following also implies that if D is an m -Dyck path of order ℓ , then $\text{rtn}(D) \in \mathcal{T}_{m\ell+2}^{(m)}$.

Proposition 14. The maps brow and rtn are inverse bijections.

Proof. The fact that brow is bijective follows from Etherington [[Eth40](#)]. Note that one can translate between the construction therein and [Definition 9](#) by using an m -generalization of the usual bijection between parenthesizations and Dyck paths.

Showing brow and rtn are inverse maps is routine. The key step is the following. Given $T \in \mathcal{T}_n^{(m)}$, suppose (i, i') is the base of an up step in $D = \text{brow}(T)$ stemming from seeing subgon Q . The path D will only pass back under the balance line which begins at (i, i') in a step that corresponds to a visit occurring after we have seen Q all $m+2$ times.

□

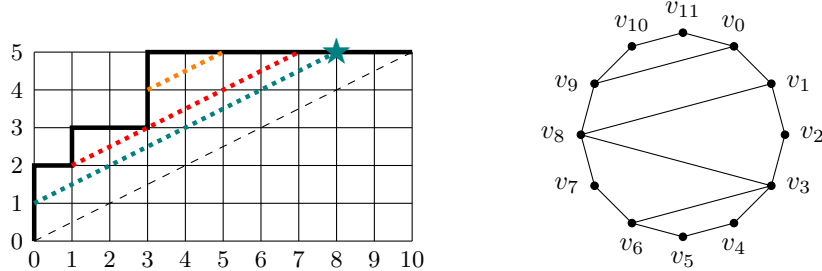


FIGURE 5. On the left, we have a 2-Dyck path of order 5 and on the right, we have the corresponding 4-angulation of a 12-gon. These are related by the maps brow and rtn .

The definition of the return map suggests how one could directly construct a frieze pattern from a Dyck path. In fact, this was recently done in the ordinary case (i.e. $m = 1$) by

²These are quite similar to paths considered in [[BPR12](#)].

Cañadas, Espinosa, Gaviria, and Rios [CGRE23]. Our result, for general m , recovers theirs when $m = 1$. First, we give two statistics on m -Dyck paths.

Definition 12. Let D be an m -Dyck path. For each $0 \leq i \leq m\ell + 1$, let $up_D(i)$ denote the number of up steps of the form $(i, j) - (i, j+1)$, $j > 0$, in D , and let $bal_D(i)$ (short for balance) denote the number of times a balance line has its first intersection with a non-corner point at a point $(i-1, j)$.

For example, in the Dyck path in Figure 5, $up_D(0) = up_D(1) = 1$, $up_D(3) = 2$, $bal_D(6) = bal_D(9) = 1$, and $bal_D(8) = 2$. Since our Dyck path is defined in the $m\ell \times \ell$ rectangle, $up_D(m\ell + 1)$ and $bal_D(0)$ are always 0. Our convention on balance lines also implies that $bal_D(1)$ is always 0.

Proposition 15. Let D be an m -Dyck path of order ℓ . The frieze pattern $F_{\text{rtn}(D)}$ satisfies

$$F_{\text{rtn}(D)}(i-1, i+1) = (up_D(i) + bal_D(i) + 1)\lambda_{m+2}$$

for all $0 \leq i \leq m\ell + 1$.

Proof. Set $T := \text{rtn}(D)$. Since T is an $(m+2)$ -angulation, following Definition 5, the value $F_T(i-1, i+1)$ is $(\deg_T(v_i) + 1)\lambda_{m+2}$ where $\deg_T(v_i)$ is the number of diagonals of T incident to v_i . There is one diagonal based at v_i for each balance line which is labeled (i, j) or (j, i) . The statistic $up_D(i)$ counts the number of the first type of balance line and the statistic $bal_D(i)$ counts the number of the second type of balance line. \square

In particular, combining Theorem 4 and Proposition 14, we have a bijection between m -Dyck paths of order ℓ and frieze patterns of type Λ_{m+2} with width $m\ell + 2$. For example, the 2-Dyck path on the left in Figure 5 is in correspondence with the frieze pattern in Figure 6. It would be interesting to find deeper connections between these combinatorial objects.

Question 4. Given an m -Dyck path D , how can one interpret $F_{\text{rtn}(D)}(i, j)$ for general $i < j$ in terms of D ?

We now have three families of objects in bijection: $(m+2)$ -angulations, finite frieze patterns of type Λ_{m+2} , and m -Dyck paths. In Lemma 6, we saw the effect that cyclic rotation of an $(m+2)$ -angulation induced on a frieze pattern. In Theorem 10, we will do the same for m -Dyck paths. We first define the proposed action.

Definition 13. Define the map

$$\widetilde{\text{rot}} : \mathcal{D}_\ell^{(m)} \rightarrow \mathcal{D}_\ell^{(m)}$$

where for $D \in \mathcal{D}_\ell^{(m)}$ the m -Dyck path, $\widetilde{\text{rot}}(D)$, is obtained by the following process:

- (1) Let $k+1$ be the position of the first R in D .
- (2) Let p_1, \dots, p_{k-1} be the first non-corner intersection points of the balance lines with labels $(0, j)$. Append a U after each R step which begins at a point p_i .
- (3) Delete the first $k+1$ letters in D . This sequence will be $U^k R$.
- (4) Prepend a U and append an R .

Remark 4. It can be convenient to rephrase part (2) of Definition 13 without appealing to the lattice path representing D . Let $D = w_1, \dots, w_d$ be an m -Dyck path and let $k+1$ be the smallest number such that $w_{k+1} = R$. Define $h : \{U, R\} \rightarrow \mathbb{Z}$ by $h(U) = m$ and $h(R) = -1$,

0	0	0	0	0	0	0	0	0	0	0	0	0	0	0	0
1	1	1	1	1	1	1	1	1	1	1	1	1	1	1	1
$2\sqrt{2}$	$2\sqrt{2}$	$\sqrt{2}$	$3\sqrt{2}$	$\sqrt{2}$	$\sqrt{2}$	$2\sqrt{2}$	$\sqrt{2}$	$3\sqrt{2}$	$2\sqrt{2}$	$\sqrt{2}$	$9\sqrt{2}$	$8\sqrt{2}$	$\sqrt{2}$	$\sqrt{2}$	$\sqrt{2}$
7	3	5	5	1	3	3	5	11	3	1	5	13	5	1	3
$5\sqrt{2}$	$5\sqrt{2}$	$7\sqrt{2}$	$4\sqrt{2}$	$2\sqrt{2}$	$\sqrt{2}$	$2\sqrt{2}$	$7\sqrt{2}$	$9\sqrt{2}$	$8\sqrt{2}$	$\sqrt{2}$	$\sqrt{2}$	$\sqrt{2}$	$\sqrt{2}$	$\sqrt{2}$	$\sqrt{2}$
7	23	11	3	3	1	9	25	13	5	1	3	3	1	3	1
$2\sqrt{2}$	$16\sqrt{2}$	$18\sqrt{2}$	$4\sqrt{2}$	$2\sqrt{2}$	$\sqrt{2}$	$2\sqrt{2}$	$16\sqrt{2}$	$18\sqrt{2}$	$4\sqrt{2}$	$2\sqrt{2}$	$\sqrt{2}$	$\sqrt{2}$	$\sqrt{2}$	$\sqrt{2}$	$\sqrt{2}$
9	25	13	5	1	3	7	23	11	3	5	5	3	3	1	1
$2\sqrt{2}$	$7\sqrt{2}$	$9\sqrt{2}$	$8\sqrt{2}$	$\sqrt{2}$	$\sqrt{2}$	$5\sqrt{2}$	$5\sqrt{2}$	$7\sqrt{2}$	$4\sqrt{2}$	$2\sqrt{2}$	$\sqrt{2}$	$\sqrt{2}$	$\sqrt{2}$	$\sqrt{2}$	$\sqrt{2}$
3	5	11	3	1	3	7	3	5	5	1	3	3	1	3	1
$\sqrt{2}$	$3\sqrt{2}$	$2\sqrt{2}$	$\sqrt{2}$	$\sqrt{2}$	$2\sqrt{2}$	$2\sqrt{2}$	$\sqrt{2}$	$3\sqrt{2}$	$\sqrt{2}$	$\sqrt{2}$	$\sqrt{2}$	$\sqrt{2}$	$\sqrt{2}$	$\sqrt{2}$	$\sqrt{2}$
1	1	1	1	1	1	1	1	1	1	1	1	1	1	1	1
0	0	0	0	0	0	0	0	0	0	0	0	0	0	0	0

FIGURE 6. The frieze pattern of type Λ_4 associated to the 4-angulation in Figure 5. One could also regard this as a frieze pattern associated to the 2-Dyck path in the same figure.

and define the *height sequence* $H_D : [d] \rightarrow \mathbb{Z}$ by $H_D(j) = \sum_{i=1}^j h(w_i)$. The m -ballot property guarantees that $H_D(j) \geq 0$ for all $j \in [d]$.

Then, the definition of $\widetilde{\text{rot}}$ can be rephrased by replacing (2) with (2') below:

(2') For each $1 \leq i \leq k-1$, let $p'_i > k$ be the smallest integer such that $H_D(p'_i) < mi$. Form a length $d + (k-1)$ binary word by placing a U at all positions $p'_i + k - i$ and filling out the remaining positions with the given Dyck word, in the same order.

Remark 5. One might expect that, when $m = 1$, $\widetilde{\text{rot}}$ coincides with *promotion* on Dyck paths. Such an action can be defined by the induced action of promotion on $2 \times n$ Standard Young Tableaux (SYT), and therefore this is another cyclic action on Dyck paths [Hai92]. One can quickly check that these actions do not agree in general though. For instance, applying promotion in this sense to the 1-Dyck path $UUURRUR$ yields $UURRUUUR$ whereas applying $\widetilde{\text{rot}}$ yields $URURUUUR$ and applying $\widetilde{\text{rot}}^{-1}$ yields $UURUURRR$.

Given $D \in \mathcal{D}_\ell^{(m)}$, consider the following operation.

- (1) Let z be the number of times D intersects the line $y = \frac{1}{m}x$, including its start point but not its end point.
- (2) Delete each of the z U 's whose starting point is on the line $y = \frac{1}{m}x$.
- (3) Delete the final R .
- (4) Prepend $U^z R$.

One can see that the above procedure is the inverse operation to $\widetilde{\text{rot}}$. In particular, $\widetilde{\text{rot}}$ is a bijection. One can rephrase this procedure, i.e. $\widetilde{\text{rot}}^{-1}$, in terms of words by noting that intersections of D with the line $y = \frac{1}{m}x$ coincide with indices where the height sequence H_D is 0.

Our final goal is to show that $\widetilde{\text{rot}}$ is the map on Dyck paths induced by rotation of m -angulations. Recall σ denotes counterclockwise rotation by $2\pi/n$ for an n -gon.

Theorem 10. *The following diagram commutes for all $\ell > 0$:*

$$\begin{array}{ccc}
\mathcal{T}_{m\ell+2}^{(m)} & \xrightarrow{\text{brow}} & \mathcal{D}_{\ell}^{(m)} \\
\sigma \downarrow & & \downarrow \widetilde{\text{rot}} \\
\mathcal{T}_{m\ell+2}^{(m)} & \xrightarrow{\text{brow}} & \mathcal{D}_{\ell}^{(m)}
\end{array}$$

Proof. Let $T \in \mathcal{T}_{m\ell+2}^{(m)}$. For each subgon Q cut out by T , let $v(Q)$ be the smallest indexed vertex incident to Q . Label the subgons incident to v_0 by Q_k, \dots, Q_1 in clockwise order, i.e., so that this indexing is opposite from the order of the visits of the browse map. In particular, v_{n-1} is a vertex on Q_k and v_1 is a vertex on Q_1 . Let r_i be such that v_{r_i+1} is the vertex with second smallest index incident to Q_i . In particular, $r_1 = 0$, and for $i > 1$, $(v_0, v_{r_i+1}) \in T$.

An m -Dyck path $D \in \mathcal{D}_{\ell}^{(m)}$ is determined by the number of up steps on each line $x = i$, i.e., the values $\text{up}_D(i)$ for all $0 \leq i \leq m\ell + 1$. From the definition of the browse map, we see that $\text{up}_{\text{brow}(T)}(i)$ is equal to the number of subgons Q cut out by T satisfying $v(Q) = v_i$. If we instead apply **brow** to the counterclockwise rotation of T , we have

$$\text{up}_{\text{brow}(\sigma(T))}(i) = \begin{cases} \text{up}_{\text{brow}(T)}(i+1) & i \neq r_j \text{ for all } j \\ \text{up}_{\text{brow}(T)}(i+1) + 1 & i = r_j \text{ for some value } j. \end{cases}$$

Now, we want to show that $\text{up}_{\widetilde{\text{rot}}(\text{brow}(T))}$ has the same relationship with $\text{up}_{\text{brow}(T)}$. Since the $\widetilde{\text{rot}}$ map deletes one initial R , we see that $\text{up}_{\widetilde{\text{rot}}(\text{brow}(T))}(i) = \text{up}_{\text{brow}(T)}(i+1)$ if there are no points p_j on the line $x = i$ in $\text{brow}(T)$ and otherwise $\text{up}_{\widetilde{\text{rot}}(\text{brow}(T))}(i) = \text{up}_{\text{brow}(T)}(i+1) + 1$.

In $\text{brow}(T)$, the intersection points p_j occur at the beginning of R steps associated to visiting the subgon Q_{j+1} at vertex v_{r_j+1} , i.e., visiting this subgon for the second time. This is true because the height sequence will only reduce by more than m after our first encounter with subgon Q_j once we have an intermediate visit at Q_{j+1} . Therefore, the condition “there are no points p_j on the line $x = i$ ” is equivalent to “ $i \neq r_j$ for all j ”, and similarly for the negation. We conclude $\widetilde{\text{rot}}(\text{brow}(T)) = \text{brow}(\sigma(T))$ since these m -Dyck paths have the same number of up steps along each vertical line. \square

Example 7. Let T be the 4-angulation displayed on the right in Figure 5 and let D be the 2-Dyck path displayed in the same figure on the left. Below, we reproduce both the Dyck path (written as a word in U 's and R 's) and the values of the height function $H_D : [d] \rightarrow \mathbb{Z}$ as defined in Remark 4.

$$\begin{array}{ll}
\text{Dyck path:} & \overbrace{U \quad U}^{v_0} \quad \overbrace{R \quad U}^{v_1} \quad \overbrace{R}^{v_2} \quad \overbrace{R \quad U \quad U}^{v_3} \quad \overbrace{R}^{v_4} \quad \overbrace{R}^{v_5} \quad \overbrace{R}^{v_6} \quad \overbrace{R}^{v_7} \quad \overbrace{R}^{v_8} \quad \overbrace{R}^{v_9} \quad \overbrace{R}^{v_{10}}
\\
H_D(j) : & 2 \quad 4 \quad 3 \quad 5 \quad 4 \quad 3 \quad 5 \quad 7 \quad 6 \quad 5 \quad 4 \quad 3 \quad 2 \quad 1 \quad 0
\end{array}$$

In Figure 7, $\sigma(T)$ is drawn on the right and $\text{brow}(\sigma(T))$ is drawn on the left. We will demonstrate that $\text{brow}(\sigma(T)) = \widetilde{\text{rot}}(D)$. The value k is 2 since the third step of D is the first right step. The intersection point p_1 is drawn as a star in Figure 5. In the language of Remark 4, $p'_i > 2$ is the smallest index such that $H(p'_i) < 2$. This occurs at the second-to-last position, i.e., $p'_i = 14$. Therefore, the 2-Dyck path $\widetilde{\text{rot}}(D)$ is the result of adding a U after the 14th step, deleting the initial subword $U^2 R$ but then reinserting an initial U , and appending

a final R . The additions are both underlined and colored in orange below.

$$\begin{array}{ccccccccc} U & U & R & & U & R & R & U & U \\ \mapsto & \cancel{U} & \cancel{U} & \cancel{R} & \cancel{U} & U & R & R & U \end{array} \quad \begin{array}{ccccccccc} R & R & R & R & R & R & R & \cancel{R} & R \\ & & & & & & & \cancel{R} & R \end{array}$$

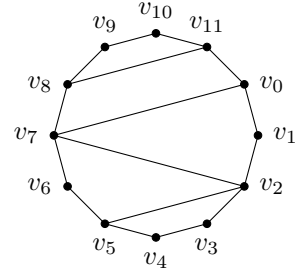
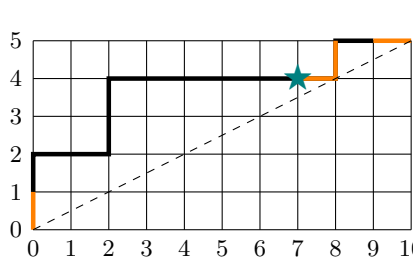


FIGURE 7. On the left, we have the altered 2-Dyck Path of order 5 given by the process in [Theorem 10](#) and on the right, we have the corresponding rotated 4-angulation of a 12-gon from [Figure 5](#).

REFERENCES

- [Bau21] Karin Baur, *Frieze patterns of integers*, Math. Intelligencer **43** (2021), no. 2, 47–54. MR 4278474
- [BBG⁺24] Karin Baur, Léa Bittmann, Emily Gunawan, Gordana Todorov, and Emine Yıldırım, *Infinite friezes of affine type d* , 2024.
- [BC21] Esther Banaian and Jiuqi Chen, *Periodic infinite frieze patterns of type $\Lambda_{p_1, \dots, p_n}$ and dissections on annuli*, 2021.
- [BCI74] D. Broline, D. W. Crowe, and I. M. Isaacs, *The geometry of frieze patterns*, Geometriae Dedicata **3** (1974), 171–176. MR 363955
- [BÇJ⁺24] Karin Baur, İlke Çanakçı, Karin M Jacobsen, Maitreyee C Kulkarni, and Gordana Todorov, *Infinite friezes and triangulations of annuli*, Journal of Algebra and its Applications **23** (2024), no. 12.
- [Bec98] David Beckwith, *Legendre polynomials and polygon dissections?*, The American mathematical monthly **105** (1998), no. 3, 256–257.
- [Bes15] Christine Bessenrodt, *Conway-Coxeter friezes and beyond: polynomially weighted walks around dissected polygons and generalized frieze patterns*, J. Algebra **442** (2015), 80–103. MR 3395054
- [BFG⁺21] Karin Baur, Eleonore Faber, Sira Gratz, Khrystyna Serhiyenko, and Gordana Todorov, *Friezes satisfying higher SL_k -determinants*, Algebra Number Theory **15** (2021), no. 1, 29–68. MR 4226982
- [BFPT19] Karin Baur, Klemens Fellner, Mark J Parsons, and Manuela Tschabold, *Growth behaviour of periodic tame friezes*, Revista Matematica Iberoamericana **35** (2019), no. 2, 575–606.
- [BK20] Esther Banaian and Elizabeth Kelley, *Snake graphs and frieze patterns from orbifolds*, Sém. Lothar. Combin. **82B** (2020), Art. 88, 12. MR 4098309
- [BPR12] François Bergeron and Louis-François Préville-Ratelle, *Higher trivariate diagonal harmonics via generalized Tamari posets*, J. Comb. **3** (2012), no. 3, 317–341 (English).
- [BPT16] Karin Baur, Mark J. Parsons, and Manuela Tschabold, *Infinite friezes*, European J. Combin. **54** (2016), 220–237. MR 3459066
- [Cay90] Cayley, *On the partitions of a polygon*, Proceedings of the London Mathematical Society **1** (1890), no. 1, 237–264.
- [CC73a] John H Conway and Harold SM Coxeter, *Triangulated polygons and frieze patterns*, The Mathematical Gazette **57** (1973), no. 400, 87–94.
- [CC73b] ———, *Triangulated polygons and frieze patterns (continued)*, The Mathematical Gazette **57** (1973), no. 401, 175–183.

- [CC06] Philippe Caldero and Frédéric Chapoton, *Cluster algebras as hall algebras of quiver representations*, Commentarii Mathematici Helvetici **81** (2006), no. 3, 595–616.
- [CCS06] P. Caldero, F. Chapoton, and R. Schiffler, *Quivers with relations arising from clusters (A_n case)*, Trans. Amer. Math. Soc. **358** (2006), no. 3, 1347–1364. MR 2187656
- [ÇFGET22] İlke Çanakçı, Anna Felikson, Ana García-Elsener, and Pavel Tumarkin, *Friezes for a pair of pants*, Sémin. Lothar. Combin. **86B** (2022), Art. 32, 12. MR 4490873
- [CGRE23] Agustín Moreno Cañadas, Isaías David Marín Gaviria, Gabriel Bravo Ríos, and Pedro Fernando Fernández Espinosa, *Coxeter’s frieze patterns arising from dyck paths*, Ricerche di Matematica **72** (2023), no. 2, 867–889.
- [Cox71] H.S.M. Coxeter, *Frieze patterns*, Acta. Arith. **18** (1971), 297–310.
- [CS14] Leonid Chekhov and Michael Shapiro, *Teichmüller spaces of riemann surfaces with orbifold points of arbitrary order and cluster variables*, International Mathematics Research Notices **2014** (2014), no. 10, 2746–2772.
- [DKK11] Kentaro Doi, Keigo Kato, and Satoyuki Kawano, *Characterization of polymer structures based on burnside’s lemma*, Physical Review E—Statistical, Nonlinear, and Soft Matter Physics **84** (2011), no. 1.
- [DR01] Satyan L. Devadoss and Ronald C. Read, *Cellular structures determined by polygons and trees*, Ann. Comb. **5** (2001), no. 1, 71–98. MR 1841954
- [EF08] Sen-Peng Eu and Tung-Shan Fu, *The cyclic sieving phenomenon for faces of generalized cluster complexes*, Advances in Applied Mathematics **40** (2008), no. 3, 350–376.
- [Eth40] IMH Etherington, *Some problems of non-associative combinations (i)*, Edinburgh Mathematical Notes **32** (1940), i–vi.
- [FP16] Bruce Fontaine and Pierre-Guy Plamondon, *Counting friezes in type D_n* , Journal of Algebraic Combinatorics **44** (2016), 433–445.
- [FR05] Sergey Fomin and Nathan Reading, *Generalized cluster complexes and Coxeter combinatorics*, Int. Math. Res. Not. **2005** (2005), no. 44, 2709–2757.
- [FT24] Anna Felikson and Pavel Tumarkin, *Friezes from surfaces and farey triangulation*, 2024.
- [FZ03] Sergey Fomin and Andrei Zelevinsky, *Cluster algebras. II. Finite type classification*, Invent. Math. **154** (2003), no. 1, 63–121. MR 2004457
- [GHL23] Antoine de Saint Germain, Min Huang, and Jiang-Hua Lu, *Friezes of cluster algebras of geometric type*, 2023.
- [GJ04] Ian P Goulden and David M Jackson, *Combinatorial enumeration*, Courier Corporation, 2004.
- [GKP94] R.L. Graham, D.E. Knuth, and O Patashnik, *Concrete mathematics. a foundation for computer science*, Addison-Wesley, New York, 1994.
- [GMV19] Emily Gunawan, Gregg Musiker, and Hannah Vogel, *Cluster algebraic interpretation of infinite friezes*, European J. Combin. **81** (2019), 22–57. MR 3949636
- [GS20] Emily Gunawan and Ralf Schiffler, *Frieze vectors and unitary friezes*, J. Comb. **11** (2020), no. 4, 681–703. MR 4164185
- [Hai92] Mark D. Haiman, *Dual equivalence with applications, including a conjecture of Proctor*, Discrete Math. **99** (1992), no. 1-3, 79–113. MR 1158783
- [HJ20] Thorsten Holm and Peter Jørgensen, *A p -angulated generalisation of conway and coxeter’s theorem on frieze patterns*, International Mathematics Research Notices **2020** (2020), no. 1, 71–90.
- [Kir57] Thomas Penyngton Kirkman, *On the k -partitions of the r -gon and r -ace*, Philosophical Transactions of the Royal Society of London (1857), no. 147, 217–272.
- [MG15] Sophie Morier-Genoud, *Coxeter’s frieze patterns at the crossroads of algebra, geometry and combinatorics*, Bulletin of the London Mathematical Society **47** (2015), no. 6, 895–938.
- [Pal08] Yann Palu, *Cluster characters for 2-Calabi-Yau triangulated categories*, Ann. Inst. Fourier (Grenoble) **58** (2008), no. 6, 2221–2248. MR 2473635
- [Pal22] Joe Pallister, *\tilde{A} and \tilde{D} type cluster algebras: triangulated surfaces and friezes*, J. Algebraic Combin. **56** (2022), no. 4, 1163–1202. MR 4496491
- [Pre23] Matthew Pressland, *From frieze patterns to cluster categories*, Modern trends in algebra and representation theory, London Math. Soc. Lecture Note Ser., vol. 486, Cambridge Univ. Press, Cambridge, 2023, pp. 109–145. MR 4619261

- [Pro20] James Propp, *The combinatorics of frieze patterns and Markoff numbers*, Integers **20** (2020), Paper No. A12, 38. MR 4067101
- [PS00] Józef H. Przytycki and Adam S. Sikora, *Polygon dissections and Euler, Fuss, Kirkman, and Cayley numbers*, J. Combin. Theory Ser. A **92** (2000), no. 1, 68–76. MR 1783940
- [RSW04] Victor Reiner, Dennis Stanton, and Dennis White, *The cyclic sieving phenomenon*, Journal of Combinatorial Theory, Series A **108** (2004), no. 1, 17–50.
- [Sag11] Bruce E. Sagan, *The cyclic sieving phenomenon: a survey*, Surveys in combinatorics 2011, London Math. Soc. Lecture Note Ser., vol. 392, Cambridge Univ. Press, Cambridge, 2011, pp. 183–233. MR 2866734
- [Sta] Dennis Stanton, personal communication.
- [Sta96] Richard P Stanley, *Polygon dissections and standard young tableaux*, Journal of Combinatorial Theory, Series A **76** (1996), no. 1, 175–177.
- [SW16] Alison Schuetz and Gwyn Whieldon, *Polygonal dissections and reversions of series*, Involve, a Journal of Mathematics **9** (2016), no. 2, 223–236.
- [WR25] N. J. Wildberger and Dean Rubine, *A hyper-Catalan series solution to polynomial equations, and the Geode*, Amer. Math. Monthly **132** (2025), no. 5, 383–402. MR 4902911

Email address: ashleigh.adams@ndsu.edu

SCHOOL OF MATHEMATICS, NORTH DAKOTA STATE UNIVERSITY, FARGO, ND 58102

Email address: esther.banaian@ucr.edu

SCHOOL OF MATHEMATICS, UNIVERSITY OF CALIFORNIA, RIVERSIDE, RIVERSIDE, CA 92521